

CAPITAL UNIVERSITY OF SCIENCE AND
TECHNOLOGY, ISLAMABAD



Determination of Potential
Inhibitors of SARS-COVID-19
Present in *Senna alexandrina*

by

Sana Javed

A thesis submitted in partial fulfillment for the
degree of Master of Science

in the

Faculty of Health and Life Sciences

Department of Bioinformatics and Biosciences

2021

Copyright © 2021 by Sana Javed

All rights reserved. No part of this thesis may be reproduced, distributed, or transmitted in any form or by any means, including photocopying, recording, or other electronic or mechanical methods, by any information storage and retrieval system without the prior written permission of the author.

I dedicate this thesis to my Parents who prayers day & night for my success.



CERTIFICATE OF APPROVAL

Determination of Potential Inhibitors of SARS-COVID-19

Present in *Senna alexandrina*

by

Sana Javed

(MBS191019)

THESIS EXAMINING COMMITTEE

S. No.	Examiner	Name	Organization
(a)	External Examiner	Dr. Sara Mumtaz	NUMS, Rawalpindi
(b)	Internal Examiner	Dr. Shaukat Iqbal	CUST, Islamabad
(c)	Supervisor	Dr. Erum Dilshad	CUST, Islamabad

Dr. Erum Dilshad

Thesis Supervisor

April, 2021

Dr. Sahar Fazal

Head

Dept. of Biosciences & Bioinformatics

April, 2021

Dr. Muhammad Abdul Qadir

Dean

Faculty of Health & Life Sciences

April, 2021

Author's Declaration

I, **Sana Javed** hereby state that my MS thesis titled “**Determination of Potential Inhibitors of SARS-COVID-19 Present in *Senna alexandrina***” is my own work and has not been submitted previously by me for taking any degree from Capital University of Science and Technology, Islamabad or anywhere else in the country/abroad.

At any time if my statement is found to be incorrect even after my graduation, the University has the right to withdraw my MS Degree.

(**Sana Javed**)

Registration No: MBS191019

Plagiarism Undertaking

I solemnly declare that research work presented in this thesis titled “**Determination of Potential Inhibitors of SARS-COVID-19 Present in *Senna alexandrina***” is solely my research work with no significant contribution from any other person. Small contribution/help wherever taken has been dully acknowledged and that complete thesis has been written by me.

I understand the zero tolerance policy of the HEC and Capital University of Science and Technology towards plagiarism. Therefore, I as an author of the above titled thesis declare that no portion of my thesis has been plagiarized and any material used as reference is properly referred/cited.

I undertake that if I am found guilty of any formal plagiarism in the above titled thesis even after award of MS Degree, the University reserves the right to withdraw/revoke my MS degree and that HEC and the University have the right to publish my name on the HEC/University website on which names of students are placed who submitted plagiarized work.

(Sana Javed)

Registration No: MBS191019

Acknowledgement

By the grace of **Allah Almighty**, the Most Beneficent, the Most Merciful, all the praises and thanks be to Allah, the Lord of the 'Alamin (mankind, jinns and all that exists), the Most Beneficent, the Most Merciful, the Only Owner of the Day of Recompense (i.e., The Day of Resurrection). I have been able to accomplish this research work and come up with final dissertation work which is necessary for the award of degree of MS in Biosciences.

The completion of this task was not easy, but it required troublesome efforts and hard work. I would like to take this opportunity to express my deepest gratitude to all those who supported and helped me during my research. After my parents' prayers there were so many peoples who have contributed to this research by support and encouragement. First and foremost, I would like to thank my mentors, Dr. Erum Dilshad and Dr. Naeem for their guidance, support, encouragement, and inspiration. I am incredibly lucky to be able to be their student and to learn from their wisdom. I sincerely appreciate them for everything that they have taught me.

I would also like to say thanks to my friends Muhammad Maaz and Arooj Wajid for helping me in the compilation of the dissertation. Further, I would like to thank the faculty members and friends in the Department of Bioinformatics and Biosciences at Capital University of Science and Technology, Islamabad.

Finally, I am thankful to Ammar Liaquat who make me realize the importance of MS and encouraged me to continue my studies. I am also thankful to my students and my colleagues who were always there for me to pray whenever I need. Due to their prayers today, I am able to accomplish my research.

Thanks to all

(Sana Javed)

Abstract

In Wuhan, China, Coronavirus Disease 2019 (COVID-19) was first detected due to a new severe acute respiratory syndrome, coronavirus 2 (SARS-CoV-2). There is no FDA approved antiviral treatment to overcome this pandemic disease. In many developed countries natural products and medicinal plants are still considered alternatives for the prevention or treatment of many diseases. *Senna alexandrina* is a small leguminous shrub of family Fabaceae that is rich source of many phytochemicals i.e., alkaloids, glycoside, carbohydrates, saponins, phenols, steroid, tannins, proteins, proteins and diterpenes. Dried fruits (beans) and leaves (dried leaflets) of that plant are used to make tablets for many diseases and fruits are mostly used make Senna infusion (tea). The 3-chymotrypsin-like protease (3CLpro) is the key protease of SARS-CoV-2, which releases replicate polyproteins during viral replication and is thus considered to be an attractive drug target. So, we reported virtual screening of 20 compounds based on molecular docking *Senna alexandrina*, those were obtained from the PubChem database. After physiochemical analysis and identification of active domains of 3CLpro, these compounds were docked via CB-Dock to determine the best potential inhibitor against COVID-19. These 20 compounds were further subjected to Lipinski rule of five and ADMET properties for drug-likeness prediction. Furthermore, the lead compound was identified with best binding affinity and pharmacological properties. Remdesivir was used as criteria for comparison. These findings suggest that the identified compound may serve as potential inhibitor against 3CLpro. The purpose of this current study is to examine the phytochemicals compounds found in *Senna alexandrina* as potential inhibitors for 3CLpro of SARS-CoV-2 by using computational approaches. However, further research is needed to investigate their potential drug uses.

Keywords: Medicinal plants, *Senna alexandrina*, 3CLpro, Phytochemicals, Antiviral drugs, Molecular docking, Proteins, Ligands.

Contents

Author's Declaration	iv
Plagiarism Undertaking	v
Acknowledgement	vi
Abstract	vii
List of Figures	x
List of Tables	xi
Abbreviations	xii
1 Introduction	1
1.1 Background	1
1.2 Problem Statement	3
1.3 Aims and Objectives	4
1.4 Scope	4
2 Literature Review	5
2.1 SARS COV-2	5
2.2 Origin	6
2.3 Discovery	7
2.4 Entry and Life Cycle	7
2.5 Symptoms	9
2.6 Treatment and Preventions	10
2.7 Statistics	10
2.8 Medicinal Plants	11
2.9 <i>Senna alexandrina</i>	12
2.9.1 Taxonomic Hierarchy	13
2.10 Molecular Docking	13
2.11 3CL Protease	14
2.12 Natural Compounds as Inhibitors of 3CL Protease	15
2.13 Inhibitors Against 3CLpro of SARS-CoV-2 in <i>Senna alexandrina</i>	16

3	Methodology	18
3.1	Selection of Disease	19
3.2	Selection of Protein	19
3.3	Analysis of Physiochemical Properties	19
3.4	Identification of Functional Domains of Target Protein	20
3.5	Ligand Preparation	20
3.6	Bioactivity Analysis of Ligands and Toxicity Measurement	21
3.7	Molecular Docking	21
3.8	Visualization of Ligand/Protein via PyMol	22
3.9	Analysis of Docked Complex via LigPlot	22
3.10	Ligand ADME Properties	22
3.11	Lead Compound Identification	23
3.12	Comparison of Antiviral Drug Against COVID-19 and Lead Compound	23
4	Results and Discussions	24
4.1	Structure of Protein	24
4.2	Analysis of Physiochemical Properties of 3CL Protease	25
4.3	Identification of Functional Domains	26
4.4	Structure of Protein Cleaned for Docking	27
4.5	Ligand Selection	27
4.6	Applicability of Lipinski Rule of Five	30
4.6.1	Toxicity Prediction of Ligands	31
4.7	Molecular Docking	36
4.8	Interaction of Ligands and Targeted Protein	37
4.9	ADME Properties of Ligands	59
4.9.1	Absorption	59
4.9.2	Distribution	60
4.9.3	Metabolism	61
4.9.4	Excretion	64
4.10	Lead Compound Identification	65
4.11	Selection of Antiviral Drug	65
4.12	ADMET Properties of Selected Drug	66
4.13	Mechanism of Action of Remdesivir	68
4.14	Remdesivir Effects on Body	68
4.15	Remdesivir Docking	69
4.16	Comparison of Remdesivir and Luteolin	70
4.16.1	Comparison of ADMET Properties	70
4.16.2	Comparison of Docking Results and Physiochemical Properties	72
5	Conclusions and Future Prospects	74
	Bibliography	75

List of Figures

2.1	Structure of SARS-CoV-2.	6
2.2	Mechanism of Entry and Life Cycle of SARS-CoV-2.	9
3.1	Flow Chart of Methodology.	18
4.1	Structure of 3Cl Protease [PDB ID 6M2Q].	24
4.2	Functional Domains of 3CL Protease.	26
4.3	Refined Structure of 3CLpro for Docking.	27
4.4	2D Representation of Docked Complex Vanillic Acid-6M2N.	38
4.5	2D Representation of Docked Complex of Benzoic Acid-6M2N	38
4.6	2D Representation of Docked Complex of Gallic Acid-6M2N	39
4.7	2D Representation of Docked Complex Cynaroside-6M2N.	39
4.8	2D Representation Docked Complex Epigallocatechin-6M2N.	40
4.9	2D Representation of Docked Complex Sennoside A-6M2N	40
4.10	2D Representation of Docked Complex Tinnevellingsucoside-6M2N.	41
4.11	2D Representation of Docked Complex Rhoifolin-6M2N.	41
4.12	2D Representation of Docked Complex Pectolarin-6M2N.	42
4.13	2D Representation of Docked Complex Syringic Acid-6M2N.	42
4.14	2D Representation of Docked Complex Baicelein-6M2N.	43
4.15	2D Representation of Docked Complex Caffeic Acid-6M2N.	43
4.16	2D Representation of Docked Complex Isoquercetin-6M2N.	44
4.17	2D Representation of Docked Complex Rhein-6M2N.	44
4.18	2D Representation of Docked Complex Kaempferol-6M2N.	45
4.19	2D Representation of Docked Complex Adenosine A-6M2N.	45
4.20	2D Representation of Docked Complex Neochlorogenic Acid-6M2N.	46
4.21	2D Representation of Docked Complex Caffeic Acid-6M2N.	46
4.22	2D Representation of Docked Complex Quercetin-6M2N.	47
4.23	2D Representation of Docked Complex Luteolin-6M2N.	47
4.24	2D Structure of Remdesivir Drug from Pubchem Database.	65
4.25	2D Representation of Remdesivir and 3CLpro.	69

List of Tables

2.1	Statistics of COVID-19 in Pakistan & worldwide.	11
2.2	Taxonomic Hierarchy of <i>Senna alexandrina</i>	13
4.1	Physiochemical Properties of 3CL protease.	25
4.2	Selected Ligands from <i>Senna alexandrina</i>	28
4.3	Selected Ligands from <i>Senna alexandrina</i>	29
4.4	Applicability of Lipinski Rule on Selected Ligands	30
4.5	Applicability of Lipinski Rule on Selected Ligands	31
4.6	A: Toxicity Prediction of Ligands.	32
4.7	B: Toxicity Prediction of Ligands.	34
4.8	Ligands with Best Binding Score Values with 3CL Protease.	36
4.9	Ligands with Best Binding Score Values with 3CL Protease.	37
4.10	Active Ligand Showing Hydrogen and Hydrophobic Interactions	48
4.11	Absorptive Properties of Ligands.	59
4.12	Absorptive Properties of Ligands.	60
4.13	Distribution Properties of Ligands.	61
4.14	Metabolic Properties of Ligands.	62
4.15	Metabolic Properties of Ligands.	63
4.16	Excretory Properties of Ligands.	64
4.17	This Table Shows Properties of Remdesivir.	66
4.18	Toxicity prediction of Remdesivir	66
4.19	Absorption values of Remdesivir.	67
4.20	Distribution Properties of Selected Drug Remdesivir	67
4.21	Metabolic Properties of Remdesivir	67
4.22	Excretory Properties of Remdesivir	67
4.23	Remdesivir Docking Scores Via Cb Dock	69
4.24	Remdesivir and Luteolin Lipinski Rule of Fives	70
4.25	Comparison of Absorptive Properties of Remdesivir and Luteolin	70
4.26	Comparison of Distribution Properties of Remdesivir and Luteolin	71
4.27	Comparison of Metabolic Properties of Remdesivir and Luteolin	71
4.28	Comparison of Excretory Properties of Remdesivir and Luteolin	71
4.29	Comparison of Toxicity of Remdesivir and Luteolin	72
4.30	Comparison of Physiochemical Properties and Docking Scores of Remdesivir and Luteolin.	73

Abbreviations

ADMET	Absorption, Distribution, Metabolism, Excretion & Toxicity
BBB	Blood brain barrier
CB-Dock	Cavity-detection guided Blind Docking
CADD	Computer-Aided Drug Designing
CASTp	Computer Atlas of Surface Topography of protein
CYP2D6	Cytochrome P450 2D6
3CLpro	3-Chymotrypsin-like protease
ERGIC	Endoplasmic reticulum-Golgi intermediate compartment
GRAVY	Grand average of hydropathy
HERG	Human Ether-a-go-go-Related Gene
HBA	Hydrogen Bond Acceptor
M.W	Molecular Weight
ORF	Open reading frame
OCT2	Organic cation transporter 2
PDB	Protein Data Bank
RdRp	RNA-dependent RNA polymerase
RDV-TP	Remdesivir Triphosphate
SARS-CoV-2	Severe acute respiratory syndrome coronavirus 2
2D	Two Dimensional
VDss	Volume of Distribution at steady state
WHO	World Health Organization
Wt-dimer	Wild-type active dimer

Chapter 1

Introduction

1.1 Background

Coronavirus 2019 (COVID-19) was caused by the Severe Acute Respiratory Syndrome Coronavirus (SARS-CoV-2) and was identified as epidemic by the World Health Organization (WHO) on March 11, 2020. As of April 12, 2020, there were more than 114,000 deaths worldwide, and more than 1.8 million people were diagnosed with this virus. The first virus appeared in respiratory tract of pneumonia patients in Wuhan, Hubei China, in December 2019 that belonged to the β coronavirus [1]. This infection could transfer from one person to another by liquid drops by cough, sneeze, hand to hand, hand to mouth, eye contact, and through touching hard surfaces.

This is systematic disease that can pass after the lungs with circulation of blood to affect muscles, kidney, liver, spleen and nervous system. Most common symptoms of COVID-19 appear in 2 to 14 days after attack of virus which include headache, muscle pain, fever, cough, loss of taste or smell and sore throat. Due to immense lung infection in many cases, emergency signs appear including difficulty in breathing due to pneumonia [2]. SARS-CoV-2 is enveloped, non-segmented and positive sense RNA virus, which belongs to sarbecovirus, ortho corona virinae subfamily that is distributed in other mammals and humans [3]. Coronaviruses

are tiny in size almost 65-125nm in diameter , size ranging from 26 to 32kbs in length, with a single-stranded RNA. The family of coronaviruses have further subgroups alpha(α), beta(β), gamma(γ) and delta (δ) coronavirus. This virus has four main structural proteins such as spike (S) glycoprotein, envelope (E) glycoprotein, membrane (M) glycoprotein and nucleocapsid (N) protein and some other proteins [4].

The enveloped viruses enter into cells by two pathways (1) a receptor-mediated pH-independent pathway in which the viral envelope fuses to start viral uncoating with the host cell membrane and (2) the pH-dependent endocytic pathway by which the virus is transferred to the endosome (low pH environment) by either clathrin or caveolin-dependent processes. [5]. The mechanism of entry of SARS-CoV-2 into the cell was first described by direct membrane fusion [6]. Although some later experiments have shown that entry of the virus can be pH-dependent [7]. There is no antiviral treatment or vaccine for animal and human coronavirus, so early detection of drug treatment is censorious for Covid-19 breakout response. Common strategies include antibiotic application, supportive care for bed rest, antiviral therapy, immunomodulating therapy, support for organ function, blood purification, respiratory support, bronchoalveolar lavage (BAL), and oxygenation of the extracorporeal membrane (ECMO) [8].

With an emergent outbreak, new transmittable disease is a novel coronavirus infection that affects all populations. SARS-CoV-2 infection has been managed as a category A infectious disease but classified as a category B infectious disease legally by the Chinese government. The most important thing is to implement infection control methods to control the source of the infection, and to prevent the transmission route and to protect the sensitive population.

The extraordinary activity of the WHO and other international government agencies has focused primarily on transmission, infection control measures, and prevention of passenger screening [9]. Many physical treatments have been used to help the patients to fight this disease but still there is no approved treatment antiviral drugs or vaccines for COVID-19, that is provoking situation. So, identification

and discovery of new effective antiviral drug is necessarily needed to overcome this corona crisis worldwide. Many natural compounds and their derivatives that have anti-inflammatory and anti-viral effects show a high binding affinity to 3-chymotrypsin-like protease (3CLpro). Computer-assisted drug discovery (CADD) have been instrumental in development of small molecules that have been therapeutically important for more than three decades, by using many computational methods such as molecular docking, screening of chemical virtual libraries performed to save money and time, resulting in faster speeds and in identification of potential drug candidates. Numerous research groups have developed interesting strategies, such as republishing existing medicines or natural products to fight COVID-19 [10]. Various traditional herbal remedies have been used, resulting in positive health effects for COVID-19 patients, especially in China [9].

Numerous attempts have been made to identify selected small molecules those have inhibitory activity against SARS-CoV-2 main proteinase, which are considered as an important potential target due to their essential role in the viral life cycle. This enzyme began to attract interest in development of drugs against SARS-CoV and was fully explored as a drug target, and many potent enzyme inhibitors have been identified [5].

1.2 Problem Statement

SARS-COVID-2 is responsible for the COVID-19 epidemic and is listed as a global health threat by the WHO due to high mortality, high primary reproduction and lack of medically approved drugs. Currently there are no approved remedies (antiviral drugs or vaccines) for COVID-19, which is the critical situation. To address this situation, we need to identify or discover new effective compounds of antivirals compounds to fight the corona crisis all around the world.

In this study, we will use many potential inhibitors of 3CLpro present in *Senna alexandrinato* conduct extensive computational studies through molecular docking.

1.3 Aims and Objectives

To predict potential inhibitors for COVID-19 by using molecular docking of natural inhibitors with 3CLpro of SARS-CoV-2 to control COVID-19.

This study requires following objectives:

- To identify potential inhibitory compounds against 3CLpro of SARS-CoV-2 present in *Senna alexandrina*.
- To perform molecular docking for checking interactions between ligand-protein complexes.
- To visualize the best interacting molecules having inhibitory effects against COVID-19.

1.4 Scope

Presently there are no approved drugs or vaccines to treat COVID-19. The genomic sequence of the SARS-CoV-2 that is responsible for COVID-19 and three-dimensional structure of main proteases are available. Importantly, inhibitors of these proteases were shown to block infection caused by SARS-CoV-2. So, it is necessary to identify potential natural compounds possessing inhibitory properties to overcome this pandemic situation. In silico molecular docking approaches would support the identification and help in exploring the potential inhibitory compounds working against the main proteases of SARS-CoV-2, which will be helpful in future for drug discovery and development of anti-viral vaccine against COVID-19.

Chapter 2

Literature Review

2.1 SARS COV-2

Coronavirus 2019 (COVID-19) was caused by the Severe Acute Respiratory Syndrome Coronavirus (SARS-CoV-2) and was identified as epidemic by the World Health Organization (WHO) on March 11, 2020. As of April 12, 2020, there were more than 114,000 deaths worldwide, and more than 1.8 million people were diagnosed with this virus. The first virus appeared in respiratory tract of pneumonia patients in Wuhan, Hubei China, in December 2019 that belonged to the β coronavirus. SARS-CoV-2 is an enveloped, positive-sense RNA virus belonging to the group Coronavirinae (Fig 2.1). A club-like projection from the surface of the virion is the special characteristic of any corona virus, a feature that mimics the corona, the crown in Latin [8]. The coronavirus has an unorganized, positive sense, a single stranded RNA genome is large (32kb) and encodes four structural and 16 non-structural proteins (NSPs). NSPs occupy two-thirds (20kb) of the viral genome, with the remaining thirds containing structural and other proteins. Spike, membrane, envelope and nucleocapsid are main structural proteins, of which M, S and E are bound to the membrane, while N is found inside the virion in the protein complex [8]. The current SARS-CoV-2 epidemic is also affecting young people and healthy people. The SARS-CoV-2 has been declared a global pandemic

in 209 countries around the world, especially among vulnerable citizens, causing a number of deaths [15].

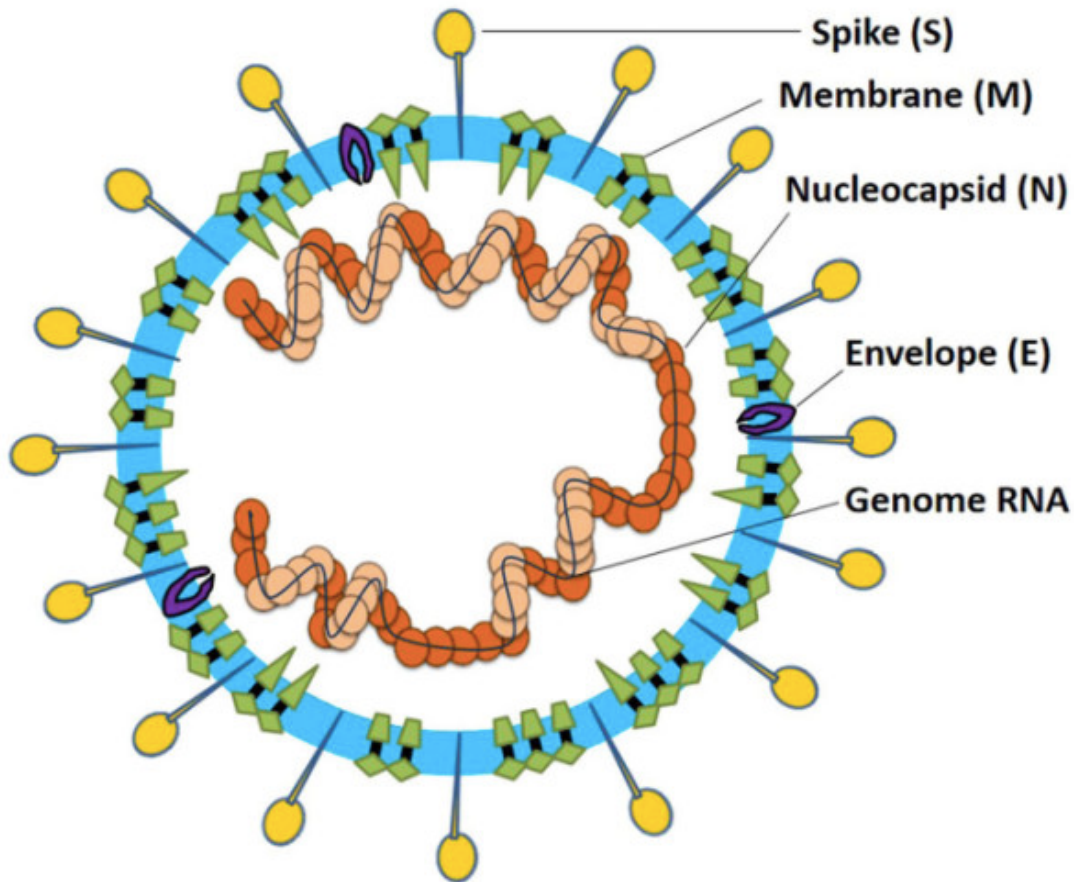


FIGURE 2.1: Structure of SARS-CoV-2.

2.2 Origin

The recent emergence of the human coronavirus SAR-CoV-2 raises many questions about evolution, including the role of species of ponds, the reintroduction of the character, and the timing of their differentiation from animal viruses. We have learned that the Sarbecoviruses virus, a virus subgenus, which includes SARS-CoV and SARS-CoV-2, is recurring and shows its genetic variation in China. [17]. Recovery means for coronaviruses that small genomic subjects can reproduce independently can be indicated if extensive sampling has been carried out in animal stocks that support co-infection, circulation, and relapse of infectious

diseases that appear to be common. SARS-CoV-2 does not in itself recover from a sarbecovirus, and its form of receptor binding is important for ACE2 receptors of humans, appears to be linked to the BAT virus and its recent recovery have not acquired through recombination. The divergence dates of deviation between BAT and SARS-CoV-2 sarbcoviruses 1948 (95% HPD (highest previous density): 1879-1999), 1982 (95% HPD: 1948-2009), 1969 (95% HPD: 1930-2000) indicates that the lineage gives rise to SAR-CoV-2 has not been observed in bats for decades [17].

2.3 Discovery

In December 2019, in the city of Wuhan (Hubei Province), a flag of pneumonia cases was epidemically linked to an open live livestock market, China told local health department officials at the Chinese Centers for Disease Control and Prevention and the World Health Organization (WHO) China Country Office. In early January, the etiological agent of pneumonia cases was found, which led to the naming of SARS-CoV-2 by an International Committee Taxonomy of Viruses (ICTV) Study Group [10]. The first available data from series puts this novel human pathogen in the Sarbecovirus subgenus as the SARS virus, which caused a global outbreak of more than 8,000 cases in 2002-2003. By mid-January 2020, the virus was spreading widely in Hubei Province, and in early March, SARA-CoV-2 was declared an epidemic [17]. SARS spread in 2002-2004 and 2012-present, respectively. The World Health Organization (WHO) declared the outbreak a pandemic on March 11th 2020, and as of July 5th , more than 11.2 million confirmed cases and 528,000 deaths had been recorded in 216 countries worldwide [18].

2.4 Entry and Life Cycle

The receptor ACE2 that is found in many organs such as the kidneys, lungs, heart and gastrointestinal tract, facilitating the entry of the virus into the target cells.

When the receptor ACE2 bind to the host cell, entering process of Coronavirus begins [15]. It is found in binding domain of the associated SARS CoV-2 receptor, KS protein, present at 331 to 524 residues, and can bind BAT ACE2 and human ACE2 strongly. After registration and binding, the process of fusion of host cell and viral membrane begins. After the fusion of type II transmembrane serine protease (TMPRSS2) present on the surface of host cell will clear the ACE2 and activate the spike-like S protein attached to the receptor.

Activation of these proteins leads to conformational changes and allows the virus to enter the cells [15]. Once SARS-CoV-2 is ingested, its genomic material will be released into the mRNA cytoplasm and translated into proteins in the nucleus. Within its genome list, the virus is made up of about 14 Open Reading Frame (ORF), each of which incorporates a variety of proteins, both formal and informal, in addition to the survival of wireless energy.

At this stage of the mutation, the same gene classes that incorporate irregular polyproteins begin to translate this process into ORF1a and ORF1b so that the two dispersed polyproteins, pp1a and pp1ab, participate in the ribosomal structure mutation [15].

Polyproteins of this viruses are supplemented by serine-type Mpro (chymotrypsin-like proteases 3CLpro) and papain-like proteases (PLpro) encoded in nonstructural protein 3 and nsp5. Most people have nsps form reflex transcriptase complexes (RTCs) in DMVs (double membrane membranes), especially RdRp (RNA-dependent RNA polymerase) and helicase containing subunits [16].

The structure and resources of small genomic proteins are translated into proteins such as S, M and E proteins into the endoplasmic reticulum and then transferred to the ERGIC (endoplasmic reticulum-Golgi intermediate compartment).

The prefabricated genome system can directly attach the N protein to the nucleocapsid form and transfer it to ERGIC. In this chamber, nucleocapsids will combine with many other structural proteins to form small purulent vesicles, found in the cell with exocytosis as shown in Fig. 2.2 [15].

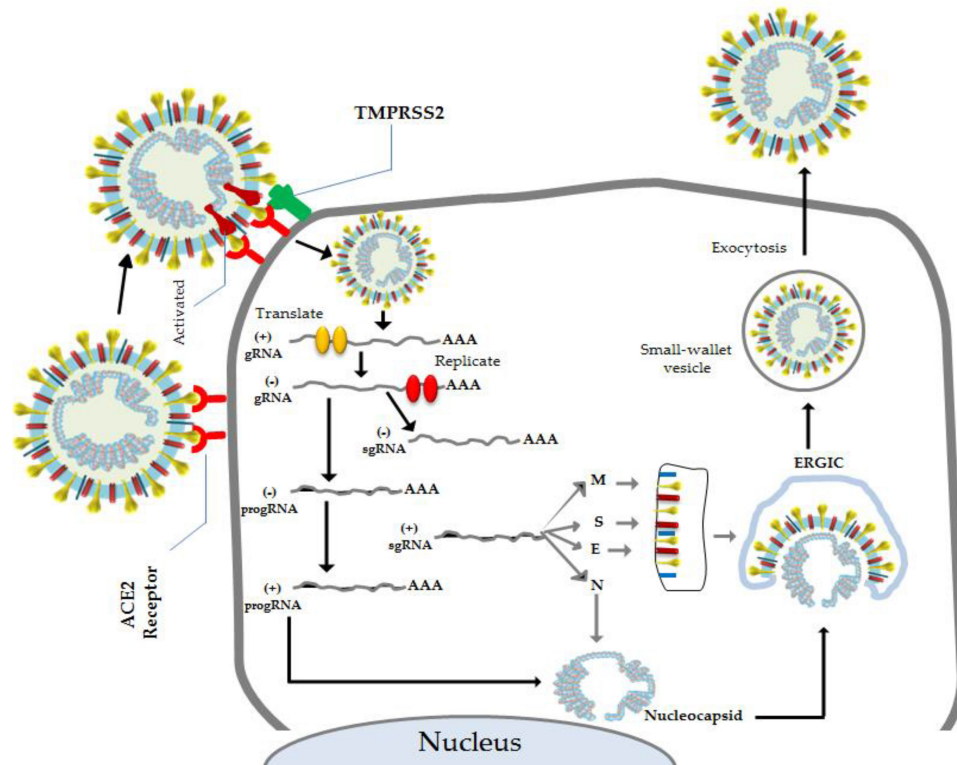


FIGURE 2.2: Mechanism of Entry and Life Cycle of SARS-CoV-2.

2.5 Symptoms

The COVID-19 affects different people in different ways. Most infected people will develop modest illness and recover without being admitted to a hospital. The symptoms of COVID-19 are not specified, and the presentation of the disease may range from asymptomatic to severe pneumonia and death. A study of 41 patients who were initially diagnosed with the spread of the disease (diagnosed date was January 2) found that the atypical symptoms include diarrhea (5%), headache (8%), hemoptysis (5%), and salivation (28%) and most common symptoms include fatigue (44%), cough (76%) and fever (98%). In 63 patients lymphocytopenia was observed. All the patients had pneumonia and complications secondary infection (10%), severe heart injury (12%) and acute respiratory distress syndrome (29%) [9]. An analysis of 1,099 confirmed cases (as of January 29) by NanShan Zhong's team found that the most common symptoms were fever (87.9%), cough (67.7%), diarrhea (3.7%) and vomiting (5.0%). Almost 25.5% of patients had at least one

primary disease (such as hypertension, chronic obstructive pulmonary disease). Lymphocytopenia was observed in 82.1 patients [16].

2.6 Treatment and Preventions

Presently, there are no antiviral treatments or vaccines for animal and human coronavirus, so it is important to discover drug as soon as possible to control COVID-19 pandemic. According to WHO a vaccine for SARS-CoV-2 should be available within 18 months, but it will require funding and public interest maintenance until the risk level is reduced [23]. The main purpose of clinical administration is largely symptomatic treatment. , With the help of organs in the intensive care of critically ill patients [20]. Common strategies include antiviral therapy, antibiotic application, bed rest-based treatment, immunomodulating therapy, respiratory support, physical activity support, bronchoalveolar lavage (BAL), extracorporeal membrane oxygenation (ECMO) and blood purification [18].

This coronavirus infection is a new communicable disease with an emerging epidemic that affects everyone. SARS-CoV-2 infection is officially classified as a B infection but is regulated by the Chinese government as an infectious disease. It is important to follow practices of infection control through controlling the origin of infection, blocking the transmission route, and protecting the sensitive population. The extraordinary activity of the WHO and other international government agencies has focused primarily on transmission, infection control measures, and prevention of passenger screening [20].

2.7 Statistics

According to last update at 2:25 pm on October 13, 2020 total cases of COVID-19 are 38,081,367 out of these 28,626,894 people recovered and 1,086,017 died. According to Pakistan's last update (<https://covid.gov.pk>) at 2:27 pm on October

13, 2020, total number of tests were reported 3,914,818 out of which 319,848 coronavirus cases were confirmed, 304,609 patients recovered (Table 2.1). Coronavirus attack rate is estimated to be 2.3 per 100000 Pakistani population [50].

TABLE 2.1: Statistics of COVID-19 in Pakistan & worldwide.

S.No	In Pakistan	WorldWide
Confirmed cases	315,727	38,081,367
Deaths	6,523	1,086,017
Recovered	300,616	28,626,894
Total tests	3,702,607	—
Critical cases	516	69,152

2.8 Medicinal Plants

The plants those have therapeutic properties or have beneficial medicinal effects on the human or animal body are called as medicinal plants. Medicinal plants have always been important sources of lead compounds in drugs. Early humans used their instincts, taste, and experience to treat their ailments. Therefore, the history of medicinal plants is as long as the history of humans [19]. Natural products and medicinal plants are still considered alternatives for the prevention or treatment of many diseases. Various traditional herbal remedies have been used, resulting in positive health effects for COVID-19 patients, especially in China [20]. Since the first days of the spread of COVID-19 in China, many traditional herbal medicines have been used. In fact, 90% of the 214 patients treated with these traditional medicines recover. Some traditional herbal remedies prevent SARS-CoV-2 infections in healthy people and improve the health of patients with mild or severe symptoms [21]. [22] studied the anti-inflammatory potential and effects of Chinese herbs known as Lianhuaqingwen (mixture of 11 medicinal species, menthol and gypsum) against SARS-CoV-2. The Chinese National Health Commission recommended herbal compounds for the treatment and management of COVID-19

[23]. [24] reviewed some medicinal plants have inhibitory effects on ACE2 receptor. They studied 141 medicinal families and purified 49 natural compounds with the ability to inhibit ACE. In addition, 16 drug species were identified to inhibit angiotensin type 1A receptors in vitro. Many flavonoids such as (Quercetin, Puerarin, Daidzein, etc.) have been tested for inhibitory effects of SARS-CoV 3CL protease activity [20].

2.9 *Senna alexandrina*

Senna alexandrina are small leguminous shrubs near Somalia, the Arabian Peninsula and the Nile. As an annual crop it stays in the field for 110-130 days. The plants soon form a mixture of 5-8 pairs of stocked oval-lanceolate leaflets (2.5 cm to 1.5 cm) and 60-70 days after sowing the calyx and flower shoots in the sub-terminal position. There is constant production. It is primarily a self-pollinating crop but can pass through beetles more (20%). Dried fruits (beans) and leaves (dried leaflets), which are used to make tablets, fruits are mostly used for making Senna infusion (tea).

The leaves are used to treat anemia, anorexia, nausea, bronchitis, heartburn, cancer, cholera, constipation, aches, pains, fevers, fungal infections, gastritis, gonorrhea, gout, hemorrhoids, hemorrhoids, Hiccups, Jaundice, Leprosy, Leukemia, Mycosis, Nausea, Neurological Disorders, Pimples, Color, Insects, Splenosis, Syphilis, Typhoid, Venereal Disease, Viral Diseases, Anti-Helminotherapy and Wound Treatment (Duke's Handbook of Medicinal Plants of the Bible) [25]. Stoll has isolated and characterized active principle of the Senna plant in 1941. First two glycosides were identified and assigned to the anthraquinone family. Many compounds were obtained from senna, such as sterol glucoside, yellow flavonol kaempferol, ascorbic acid, resin, mucilage polysaccharides and calcium oxalate [26].

The main phytochemicals present in *Senna alexandrina* are carbohydrates, alkaloids, glycosides, saponins, tannins, phenols, flavonoids, steroids, proteins and amino acids and diterpenes [25].

2.9.1 Taxonomic Hierarchy

Senna alexandrina is part of the Fabaceae family (Table 2.2), Caesalpinioideae is natively distributed in the tropics and subtropical regions (Mexico, Africa, Pakistan, Saudi Arabia, India and others), with over 260 (350) species of shrubs and herbs and some species also found in hot regions [25].

TABLE 2.2: Taxonomic Hierarchy of *Senna alexandrina*

S.No	Domains	Eukarya
1	Kingdom	Plantae
2	Sub Kingdom	Viridiplantae
3	Infrakingdom	Streptophyta
4	Super Division	Embryophyta
5	Division	Tracheophyta
6	Sub Division	Spermatophytina
7	Class	Magnoliopsida
8	Super Order	Rosanae
9	Family	Fabaceae
10	Genus	Senna
11	Species	<i>Senna alexandrina</i> Mill

2.10 Molecular Docking

Molecular Docking is technique used to estimate the strength of a bond between a ligand and a target protein through a special scoring function and to determine the correct structure of the ligand within the target binding site. The 3D structure of the target proteins and the ligands is taken as the input for docking. It represents a frequently used approach in structure-based drug design since it requires 3D structure of a target protein. It can be used to determine the correct structure of the ligand within the target binding site, and to estimate the strength of the binding between the ligand and the target proteins through a specific scoring function [22]. Each docking program uses one or more specific search algorithms, one of which is used to predict possible compliance with the receptor-ligand complex [23]. Currently, molecular docking is becoming a key tool for drug discovery and

molecular modeling applications. The reliability of molecular docking depends on the accuracy of the scoring function, which can guide the ligand pose and determine when thousands of possible lines can be generated. [24]. In addition, there are some tools like Dock, Gold, Flex X-One ICM that are mainly used for high docking inclusion [25].

Molecular docking can reveal the viability of any biochemical reaction that is performed before the experimental part of an investigation. Particularly, the interaction between small molecules (ligands) and protein targets (which may be an enzyme) may predict inhibition or activation of an enzyme. This type of information can provide raw material for drug designing [26].

2.11 3CL Protease

It is an important protease present in coronaviruses that cleaves the polyprotein of corona virus at eleven conserved sites. This is cysteine protease and has cysteine histidine catalytic dyad at its active site and cleaves a Gln-(Ser / Ala / Gly) peptide bond [27]. 3CLpro can cleave a peptide bond present between glutamine at the P1' position and a small amino acid (serine, alanine or glycine) at the P1' position. In common parlance, "3C" refers to 3C proteases (3Cpro), a homologous protease found in picornaviruses. This protease is important in the processing of corona virus replication polyprotein (P0C6U8). This is the main protease in coronaviruses which corresponds to nonstructural protein 5 (nsp5) [28]. 3CLpro of SARS-CoV-2 cleaves at 11 sites in the polyproteins to produce individual functional proteins including as an RNA-dependent RNA polymerase, a helicase, a single-stranded RNA-binding protein, an exoribonuclease, an endoribonuclease, and a 2'-ribose methyltransferase. It is a cysteine protease derived from polyproteins and through its proteolytic activity it forms a homodimer with one active site per subunit [29].

There are three types of crystal structures of SARS-CoV 3CLpro as Wild-type active dimer (Wt-dimer), Monomeric forms or the G11A, R298A, and S139A mutants and highly active octamer. 3CLpro consist of N-terminal finger, catalytic

domain and C-terminal domain with residues 1-8, 8-84 and 201-306 respectively, and overall structural domains are similar as all of the reported 3CLpro structure [30].

2.12 Natural Compounds as Inhibitors of 3CL Protease

In the last 5 years, several inhibitors have been introduced on the basis of crystal structure of 3CL protease. Several inhibitors of 3CLpro have been studied such as small molecule and peptide mimetics. Major studies focused primarily on small molecular compounds which confirm the crystal structure of 3CLpro through virtual screening bases and effects of inhibitory compounds on enzyme activity in vitro [31]. Tetrapeptide inhibitor 3 (IC₅₀ =98 nm) and D0-serine derivative 4 from serine were designed and screened against SARS-CoV 3CL RI mutant protease [32]. For identifying inhibitory effects on SARS-CoV 3CLpro, many flavonoids which contain 10 different scaffolds was experimented in vitro. In these compounds, significant inhibitory effects of herbacetin, rhoifolin and pectolinarin were found having IC₅₀ values of 27.5, 33.2 and 37.8 uM respectively [33]. Many alkylated chalcones isolated from *Angelica keiskei* were tested for their preventing activities against 3CLpro of SARS-CoV [34]. Some derivatives of pyrazolone were synthesized and virtually screened against 3CLpro SARS-CoV-2. The strongest inhibition (IC₅₀ of 5.8 ± 1.5 uM) was shown by compound 18 which contain pyrazolone rings with three hydrophobic. The carboxylate in ring A and phenyl pharmacophore in ring C were important for the inhibition of 3CL protease [35]. On the basis of specific computer-assisted drug design, Michael acceptor N3 31 is a powerful inhibitor of 3CLpro that fits inside the substrate binding of enzyme [36]. A compound isoflavone (32) was obtained from *Psoralea argbborescens*. According to molecular dynamic simulations and homology modelling, this compound 32 form H-bonds with the His41 and Cys145 catalytic dyad of SARS-CoV-2 3CLpro with a docking score of 16.35kcal/mol [37]. An ethanol extract obtained

from *Torreya nucifera* leaves showed good SARS-CoV 3CLpro inhibitory activity (62% at 100 ug/mL) [38]. Some compounds extracted from *Ecklonia cava* as phlorotannins 8 and bieckol (38) form H-bonds with Cys145 and His41 residues of SARS-CoV-2 with binding scores of -12.1kcal/mol and 12.9kcal/mol respectively. Both compounds exhibited inhibitory activity against 3CLpro of SARS-CoV-2 [39].

Some anti-malarial drug chloroquine and hydroxychloroquine have been reported to have some therapeutic effect against COVID-19. By considering the various pharmaceutical properties of the natural products, 17 compounds; hesperidin, demethoxycurcumin, curcumin, Epigallocatechin gallate (EGCG), epigallocatechin (EGC), puerarin, myricitrin, scutellarin, capsaicin, vitexin, quercitrin, ursolic acid, apiin, glabridin, rhoifolin, glycyrrhizin and rutin were studied for their inhibitory activity against 3CLpro of SARS-CoV-2. Tipranavir, indinavir, azidothymidine and saquinavir were best anti-viral drugs, although diethylcarbamazine, mepacrine, primaquine, artemisinin and niclosamide were screened for their inhibitory activities and those were anti-nematodes [40].

2.13 Inhibitors Against 3CLpro of SARS-CoV-2 in *Senna alexandrina*

The naturally occurring substances are those have antiviral activities, could inhibit the activity of 3CLpro of SARS-CoV-2 potentially and have minimal side effects, low toxicity, anti-pathogenic effects, and most importantly are readily available. The leaf extracts of *Senna alexandrina* obtained as a crude extract have potential as antimicrobial agent. Standard phytochemical analysis of extract of *Senna* leaves finds that phytochemical constituents like Phenols, Flavonoids, Alkaloids Carbohydrates, Glycosides, Tannins and Saponins [41]. The most effective substance Sennaglucosides is naturally occurring substance that is obtained from *Senna alexandrina*. Their leaves are used for many medicinal purposes such as in treatment of constipation and have a powerful laxative effect. They also showed

inhibitory effects against 3CLpro of SARS-CoV-2. Naringin also have inhibition properties against 3CLpro [42]. Some other natural compounds i.e. sennoside A, sennoside B also show inhibitory effects against SARS-CoV-2 [43].

Chapter 3

Methodology

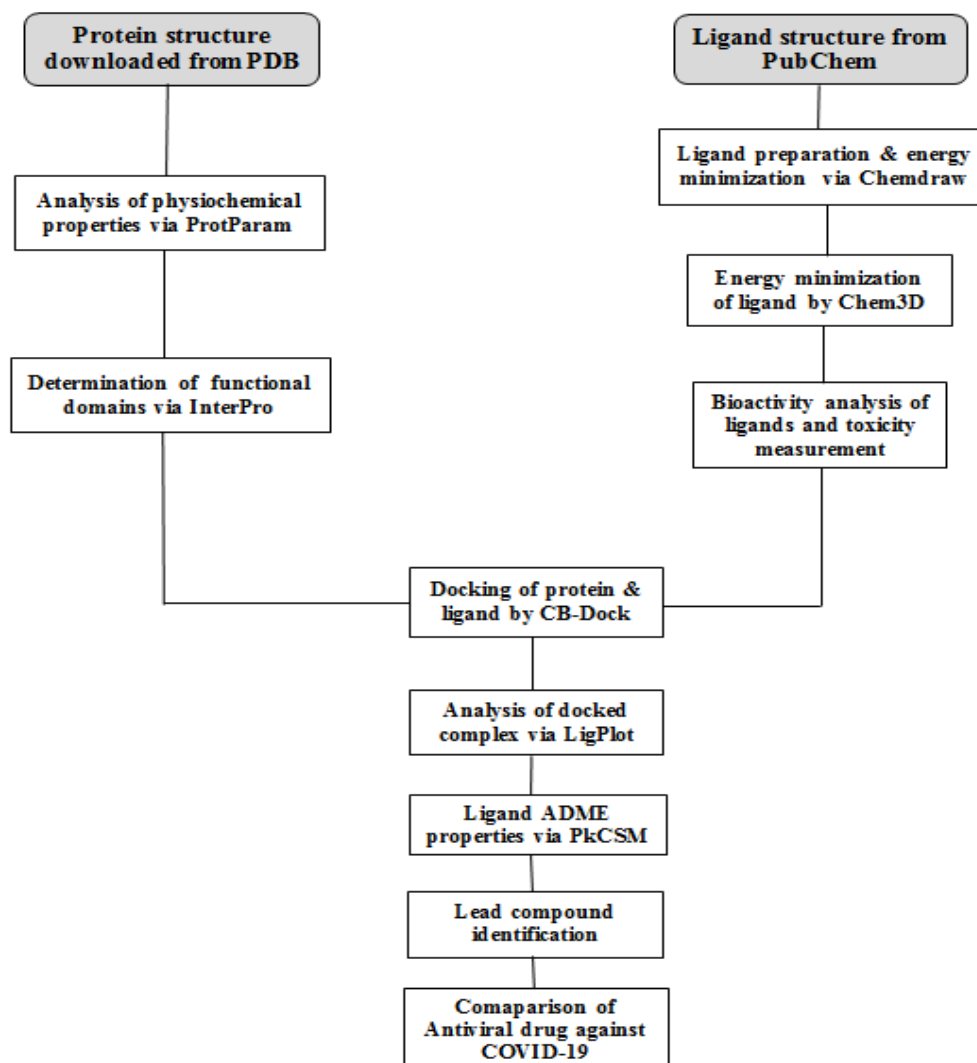


FIGURE 3.1: Flow Chart of Methodology.

3.1 Selection of Disease

COVID-19 that is caused by coronavirus, called SARS-CoV-2, was identified by the WHO as an epidemic. The rapidly evolving COVID-19 epidemic has unprecedented level of global public health. Therefore, a vaccine or drug to control SARS-CoV-2 is urgently needed. After infection, the single stranded RNA genome of SARS-CoV-2 is translated into large polyproteins that after further processing, form a viral replication complex based on virus-specific proteases in various non-synthetic proteins, main proteases (3-CL proteases) and papain proteases. This essential function of important proteases in replication of virus is a promising target for potential treatment of novel coronavirus infections [18].

3.2 Selection of Protein

Structure of 3CLpro of SARS-CoV-2 will be obtained from Protein Data Bank (PDB ID: 6M2Q) in pdb format. PDB archive is the only source of information about the 3D structure of large biological molecules, including nucleic acids and proteins. If the 3D structure of the protein is not available in the PDB, the protein will be obtained by I-TASSER through submitting the sequence of the targeted protein in the FASTA format. I-Tasser server is designed to automatically predict the structure of full-length 3D proteins. I-Tasser server output for all queries included up to five full-length models, the confidence scores, standard deviation of estimations and estimated TM scores and RMS [44].

3.3 Analysis of Physicochemical Properties

Physicochemical properties play a significant role in determining the function of proteins. ProtParam will be used to predict these properties of 3CL protease under Accession No. [A0A6C0M8P6-SARS2]. In physicochemical parameters of

selected protein 3CLpro of SARS-CoV-2, Mol.weight, atomic composition, isoelectric point, no. of amino acids, instability index, grand average of hydropathicity (GRAVY), No. of negatively charged residues (Asp + Glu), No. of positively charged residues (Arg + Lys), Aliphatic index, and amino acid and atomic composition are included, and these properties will be investigated using the ProtParam ExPASy tool [52].

3.4 Identification of Functional Domains of Target Protein

InterPro provides effective protein analysis by separating them from families and predicting domains and active sites. To classify proteins, InterPro uses predictive forms, called as signatures, using a variety of information (known as member databases) and provided an Interprofessional Consortium [46]. InterPro (<https://www.ebi.ac.uk/interpro/>) has been used to identify active domains of 3CLpro domains.

3.5 Ligand Preparation

The 3-dimensional (3D) structure of ligands will be obtained from PubChem. The PubChem is the world's largest repository of freely accessible chemical information database. We can search number of ligands by their names, molecular formula, structure and by other information [45].

If targeted structure is not available PubChem, then it will be drawn via ChemDraw by inserting Canonical smileys derived from PubChem. MM2 Energy minimization will be identified by Chem3D ultra then Ligand structure will be downloaded in .sdf form.

3.6 Bioactivity Analysis of Ligands and Toxicity Measurement

Selected ligands from PubChem database follow the Lipinski rule of five, that is a rule to evaluate drug likeness or determination of chemical compound with a certain pharmacological or biological activity has chemical properties and physical properties that would make it a likely orally active drug. The potential success of a compound depends on its ADMET properties. PkCSM (<https://omictools.com/pk-csm-tool>) is an online tool that helps to find the ADMET properties of compounds [54]. The rules are as follows:

- The logP value of most “drug-like” molecules should be limited to 5.
- Molecular weight should be under 500.
- Maximum number of H-bond acceptor should be 10.
- Maximum number of H-bond donor should be 5.

3.7 Molecular Docking

Molecular Docking is technique used to estimate the strength of a bond between a ligand and a target protein through a special scoring function and to determine the correct structure of the ligand within the target binding site. The 3D structure of the target proteins and the ligands is taken as the input for docking. It represents a frequently used approach in structure-based drug design since it requires 3D structure of a target protein. Molecular docking of protein and ligand will be done through Cavity-detection guided Blind Docking (CB-Dock). CB-Dock is a method of protein ligand docking that is used to identify binding sites, calculates the size and center automatically and personalize the docking box size and perform the molecular docking through AutoDock Vina [47]. Upload 3D structures of protein (.pdb) and ligand (.sdf) and submit to start docking. CB-Dock will provide an

interactive 3D visualization of results in 5 different poses. Best pose will be selected on basis of minimum vina score given in (kJ/m-1).

3.8 Visualization of Ligand/Protein via PyMol

Docked complex of ligand and protein will visualized by PyMol. It is a free open source of molecular visualization that can produce high-quality 3D images of proteins, small molecules, nucleic acids, and electron densities etc. This is capable of editing molecules, ray tracing and making movies [48]. Docking poses generated via CB-Dock will visualized and save as a molecule in in .pdb form in one file for further analysis.

3.9 Analysis of Docked Complex via LigPlot

Analysis of docked complex (.pdb) will done by LigPlot, that generates automatically schematic diagram of protein ligand interactions for given PDB file. These interactions are modified through hydrophobic contacts and hydrogen bonds. In Computational biology, LigPlot generates schematic 2D representations of protein-ligand complex, which facilitates the rapid examination of many enzyme complexes and demonstrates an informative and simple representation of the intermolecular interactions, these includes hydrophobic interactions, hydrogen bonds and atom accessibilities [48].

3.10 Ligand ADME Properties

In early stage of drug development ADME properties is done to eliminate weak drug that allow us to focus on potential drug. The compounds were further screened on the basis of drug score, drug-likeness and toxicity. Determination

of the ADME (Absorption, Distribution, Metabolism, and Excretion) properties of the drug molecule will be done by using PkCSM [53].

3.11 Lead Compound Identification

After a detailed analysis of protein and ligand interactions, docking scores and toxicity studies, the most active inhibitor was identified. The selected compound is our lead compound [54].

3.12 Comparison of Antiviral Drug Against COVID-19 and Lead Compound

The existing literature does not currently provide conclusive evidence against the use of antiviral drugs in the treatment of COVID-19 patients. Although some clinical trials suggest that some antiviral drugs may speed up recovery time and some corticosteroids may be beneficial if used in the early acute phase of infection [55].

Chapter 4

Results and Discussions

4.1 Structure of Protein

The structure of 3CLpro that is available in PDB was shown in Figure 4.1.

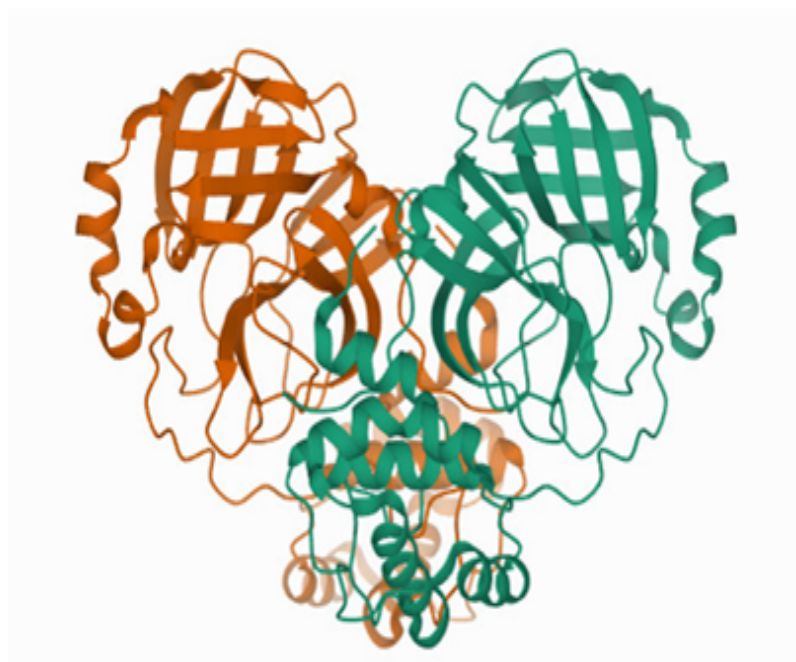


FIGURE 4.1: Structure of 3CL Protease [PDB ID 6M2Q].

4.2 Analysis of Physiochemical Properties of 3CL Protease

ProtParam is the tool that was used to find out various chemical and physical parameters of selected protein. The determined parameters are molecular weight, amino acid composition, theoretical pI, estimated half-life, atomic composition, aliphatic index, instability index, extinction coefficient, and grand average of hydropathicity (GRAVY) [56]. Physiochemical properties of 3CLpro were shown in Table 4.1.

TABLE 4.1: Physiochemical Properties of 3CL protease.

S No	Parameters	SARS-CoV-2 3CLpro
1	M.W	33796.64 Dalton
2	No. of amino acids	306
3	Theoretical pI	62
4	Instability index (II)	27.65 (stable)
5	No. of negatively charged residues (Asp + Glu)	26
6	No. of positively charged residues (Arg + Lys)	22
7	Aliphatic index	82.12
8	Grand average of hydropathicity (GRAVY)	-0.019
9	Atomic composition	Carbon-1499; Hydrogen-2318; Nitrogen-402; Oxygen-445; Sulfur-22
10	Total number of atoms	4686
11	Amino acid composition	Ala-17 (5.6%); Arg-11 (3.6%); Asn-21 (6.9%); Asp-17 (5.6%); Cys-12 (3.9%); Gln-14 (4.6%); Glu-9 (2.9%); Gly-26 (8.5%); His-7 (2.3%); Ile-11 (3.6%);

Leu-29 (9.5%); Lys-11 (3.6%);
Met-10 (3.3%); Phe-17 (5.6%);
Pro-13 (4.2%); Ser-16 (5.2%);
Thr-24 (7.8%); Trp-3 (1.0%);
Tyr-11 (3.6%); Val-27 (8.8%);
Pyl-0 (0.0%); Sec-0 (0.0%)

MW indicate (Molecular weight), pI indicates (Theoretical pI), NR indicate total number of negatively charged residues (Asp + Glu), PR indicate total number of positively charged residues (Arg + Lys), II indicate (instability index), AI indicate (Aliphatic index) and GRAVY indicate (Grand average of hydrophaticity).

4.3 Identification of Functional Domains

Many proteins consist of several functional domains which are active parts of protein involved in interactions of proteins with other substances [57]. In the case of 3CL protease of SARS-CoV-2 domains I, II and III consist of residues 1-8 and 8-184 and 201-306, respectively. Figure 4.2 shows functional domains of 3CLpro as N-terminal finger (residues 1-8), Catalytic domain (residues 8-184) and C-terminal finger domain (residues 201-306).

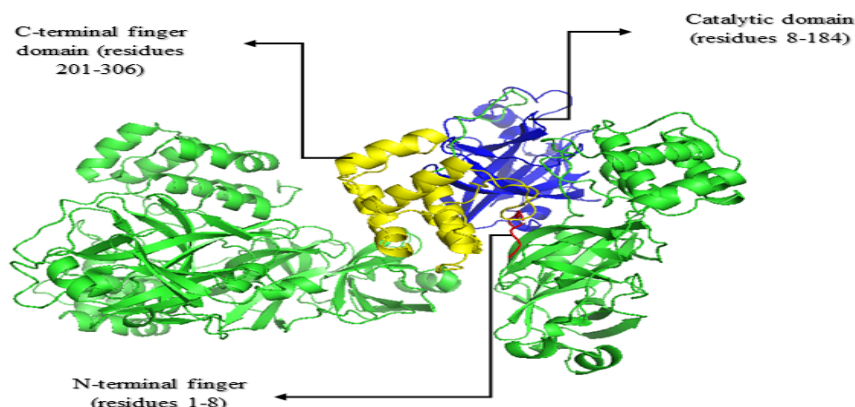


FIGURE 4.2: Functional Domains of 3CL Protease.

4.4 Structure of Protein Cleaned for Docking

The selected protein is refined in PyMol which will be used in molecular docking. Figure 4.3 shows refined 3D structure of 3CL protease.

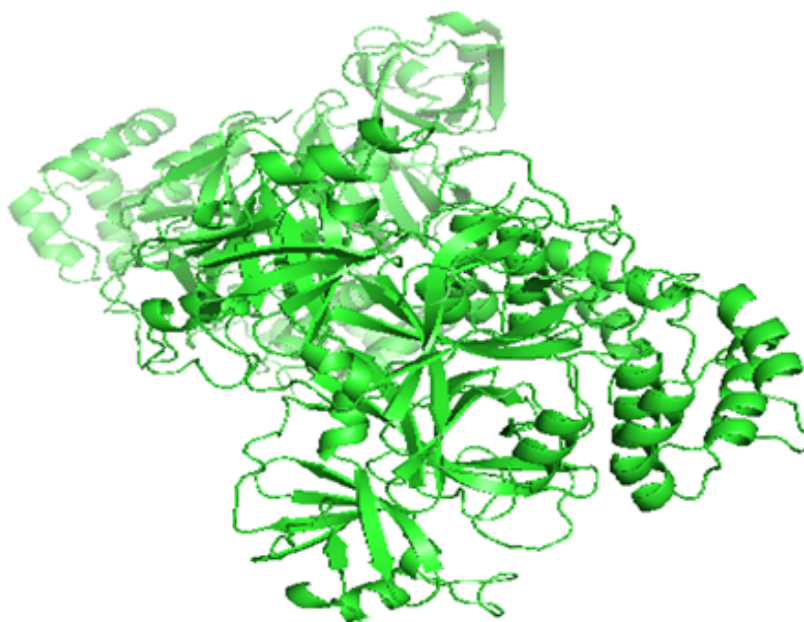


FIGURE 4.3: Refined Structure of 3CLpro for Docking.

4.5 Ligand Selection

The discovery of 3CLpro structure in SARS-CoV-2 provides a great opportunity to identify potential drug candidates for treatment of COVID-19. The coronavirus replication is controlled by viral 3CLpro and it is required for its life cycle so, it is proved as promising drug discovery target for SARS-CoV-2 [58]. Several bioactive compounds obtained from *Senna alexandrina* show potential targets for 3CLpro of SARS-CoV-2. Selected ligands along with their molecular weight and structure were shown in Table 4.2 & 4.3 respectively. All inhibitory compounds were obtained from Pubchem and we used ChemD for energy minimization of these compounds as Gallic acid 10.7638 kcal/mol, Rhein 25.921 kcal/mol, Luteolin -7,7602 kcal/mol and Isoquercetin 35.224 kcal/mol.

TABLE 4.2: Selected Ligands from *Senna alexandrina*.

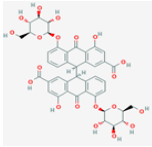
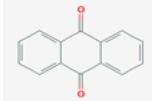
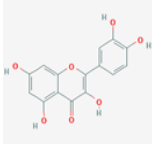
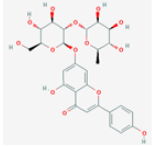
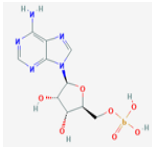
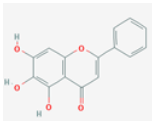
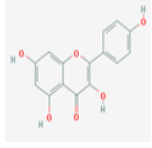
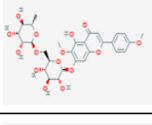
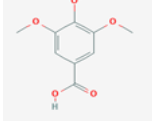
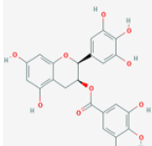
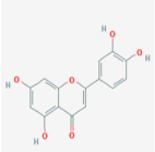
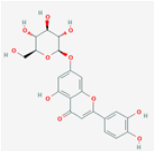
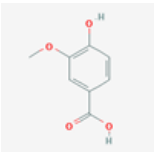
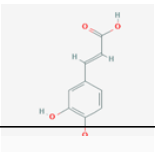
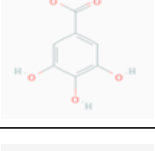
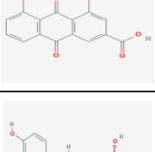
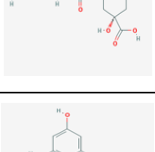
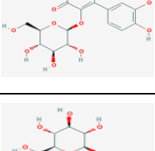
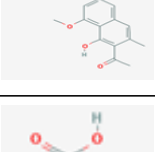
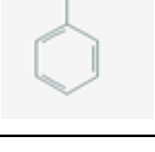
S.No	Compounds	Molecular Formula	Molecular Weight	Structure
1	Sennoside A	$C_{42}H_{38}O_{20}$	862.70 g/mol	
2	Anthraquinone	$C_{14}H_8O_2$	208.210 g/mol	
3	Quercetin	$C_{15}H_{10}O_7$	302.23 g/mol	
4	Rhoifolin	$C_{27}H_{30}O_{14}$	578.500 g/mol	
5	Adenosine A	$C_{10}H_{14}N_5O_7P$	347.220 g/mol	
6	Baicalein	$C_{15}H_{10}O_5$	270.240 g/mol	
7	Kaempferol	$C_{15}H_{10}O_6$	286.240 g/mol	
8	Pectolinari	$C_{29}H_{34}O_{15}$	622.600 g/mol	
9	Syringic acid	$C_9H_{10}O_5$	198.170 g/mol	
10	Epigallocatechin	$C_{22}H_{18}O_{11}$	458.400 g/mol	

TABLE 4.3: Selected Ligands from *Senna alexandrina*.

S.No	Compounds	Molecular Formula	Molecular Weight	Structure
11	Luteolin	$C_{15}H_{10}O_6$	286.239 g/mol	
12	Cynaroside	$C_{21}H_{20}O_{11}$	448.400 g/mol	
13	Vanillic acid	$C_8H_8O_4$	168.15 g/mol	
14	Caffeic acid	$C_9H_8O_4$	180.16 g/mol	
15	Gallic acid	$C_7H_6O_5$	170.120 g/mol	
16	Rhein	$C_{15}H_8O_6$	284.220 g/mol	
17	Neochlorogenic acid	$C_{16}H_{18}O_9$	354.310 g/mol	
18	Isoquercetin	$C_{21}H_{20}O_{12}$	464.400 g/mol	
19	Tinnevellin glucoside	$C_{20}H_{24}O_9$	408.4 g/mol	
20	Benzoic acid	$C_7H_6O_2$	122.120 g/mol	

4.6 Applicability of Lipinski Rule of Five

Safety is the most important issue during drug development, including variety of toxicities and unfavorable drug effects, which should be assessed in preclinical and clinical phases [59]. PkCSM (<https://omictools.com/pkcsm-tool>) is an online tool that was used to find Lipinski properties. According to that rule, the log p value of molecule should be limited to 5, molecular weight should be less than 500, maximum number of H bond acceptors should be 10 and maximum number of H bond donors should be 5 [60]. All of selected ligands follow Lipinski rule of five except Sennoside A, Rhoifolin, and Pectolinarin shown in Table 4.4 & 4.5.

TABLE 4.4: Applicability of Lipinski Rule on Selected Ligands

S.No	Ligands	logP Value	Molecular Weight	H-Bond Acceptor	H-bond Donor
1	Sennoside A	862.746	-1.0956 g/- mol	18	12
2	Anthraquinone	208.216	2.462 g/mol	2	0
3	Quercetin	302.238	1.988 g/mol	7	5
4	Rhoifolin	578.523	-1.0983 g/- mol	14	8
5	Adenosine A	347.224	-1.863 g/mol	10	5
6	Baicelein	270.24	2.5768 g/mol	5	3
7	Kaempferol	286.239	2.2824 g/mol	6	4
8	Pectolinarin	622.576	-0.7867 g/- mol	15	7
9	Syringic acid	198.174	1.1076 g/mol	4	2
10	Epigallocatechin	306.27	1.2517 g/mol	7	6

TABLE 4.5: Applicability of Lipinski Rule on Selected Ligands

S.No	Ligands	logP Value	Molecular Weight	H-Bond Acceptor	H-bond Donor
11	Luteolin	286.239	2.2824 g/mol	6	4
12	Cynaroside	448.38	-0.2445 g/mol	10	7
13	Caffeic acid	180.16	1.1956 g/mol	3	3
14	Gallic acid	170.12	0.501 g/mol	4	4
15	Neochlorogenic acid	354.311	-0.6459 g/mol	8	6
16	Isoquercetin	464.379	-0.5389 g/mol	9	8
17	Benzoic acid	122.123	1.3848 g/mol	1	1
18	Tinnevellin glucoside	408.403	0.2437 g/mol	9	5
19	Rhein	284.223	1.5714 g/mol	5	3
20	Vanillic acid	168.148	1.099 g/mol	3	2

4.6.1 Toxicity Prediction of Ligands

PkCSM is the online tool which was used to find the toxicity of selected compounds. This online tool which provides an integrated platform to rapidly evaluate pharmacokinetic and toxicity properties of a drugs. The toxicity values of ligands against 3CLpro were shown in Table 4.6A and 4.7B.

TABLE 4.6: A: Toxicity Prediction of Ligands.

S.No	Ligands	Max. tolerated dose(human) mg/Kg	hERG I inhibitor	hERG II inhibitor	Oral Rat Acute toxicity mol/Kg	Oral Rat Chronic toxicity mg/Kg
1	Adenosine	0.848	No	No	1.864	3.366
2	Sennoside A	0.449	No	No	2.482	8.211
3	Rhoifolin	0.492	No	Yes	2.498	4.443
4	Quercetin	0.499	No	No	2.471	2.612
5	Baicelein	0.498	No	No	2.325	2.645
6	Kaempferol	0.531	No	No	2.449	2.505
7	Pectolarin	0.543	No	Yes	2.521	3.382
8	Syringic acid	1.374	No	No	2.157	2.415
9	Epigallocatechin	0.506	No	No	2.27	2.927
10	Luteolin	0.499	No	No	2.455	2.409

Continued Table 4.6 A: Toxicity Prediction of Ligands.

S.No	Ligands	Max. tolerated dose(human) mg/Kg	hERG I inhibitor	hERG II inhibitor	Oral Rat Acute toxicity mol/Kg	Oral Rat Chronic toxicity mg/Kg
11	Cynaroside	0.584	No	No	2.547	4.279
12	Anthraquinone	0.291	No	No	1.979	2.219
13	Gallic acid	0.7	No	No	2.218	3.366
14	Neochlorogenic acid	-0.134	No	No	1.973	2.982
15	Isoquercetin	0.569	No	Yes	2.541	4.417
16	Benzoic acid	0.612	No	No	2.17	2.637
17	Tinnevellin glucoside	0.206	No	No	2.294	3.638
18	Rhein	0.716	No	No	2.533	2.208
19	Vanillic acid	0.719	No	No	2.454	2.032
20	Caffeic acid	1.145	No	No	2.383	2.092

TABLE 4.7: B: Toxicity Prediction of Ligands.

S.No	Ligands	Hepatotoxicity	Skin Sensation	t. pyriformis toxicity log ug/L	Minnow toxicity log mM
1	Adenosine	No	No	0.285	3.612
2	Sennoside A	No	No	0.285	14.648
3	Rhoifolin	No	No	0.2853	3.865
4	Quercetin	No	No	0.288	3.721
5	Baicelein	No	No	0.42	1.25
6	Kaempferol	No	No	0.312	2.885
7	Pectolinarin	No	No	0.285	5.349
8	Syringic acid	No	No	0.281	2.554
9	Epigallocatechin	No	No	0.286	4.235
10	Luteolin	No	No	0.326	3.169

Continued Table 4.7 B: Toxicity Prediction of Ligands.

S.No	Ligands	Hepatotoxicity	Skin sensation	t. pyriformis toxicity log ug/L	Minnow toxicity log mM
11	Cynaroside	No	No	0.285	6.342
12	Anthraquinone	No	Yes	1.29	1.032
13	Gallic acid	No	No	0.285	3.188
14	Neochlorogenic acid	No	No	0.285	5.741
15	Isoquercetin	No	No	0.285	8.061
16	Benzoic acid	No	No	0.087	1.838
17	Tinnevellin glucoside	No	No	0.285	4.085
18	Rhein	No	No	0.285	2.547
19	Vanillic acid	No	No	0.265	1.926
20	Caffeic acid	No	No	0.293	2.246

4.7 Molecular Docking

Molecular Docking is a technique used to estimate the strength of a bond between a ligand and a target protein through a special scoring function and to determine the correct structure of the ligand within the target binding site. The 3D structure of the target proteins and the ligands is taken as the input for docking. Molecular docking of protein and ligand was performed through Cavity-detection guided Blind Docking (CB-Dock). Protein ligand docking is a powerful tool for computer-aided drug discovery (CADD) [61]. An interactive 3D visualization of results in 5 different poses were obtained via CB-Dock. Best pose was selected on basis of minimum vina score given in (kJ/m-1). Ligands with best binding scores were shown in Table 4.8 and 4.9.

TABLE 4.8: Ligands with Best Binding Score Values with 3CL Protease.

S.No	Ligands	Binding Score (kJ/m-1)	Cavity size	Grid Map	HBA
1	Sennoside A	-11.3	4410	5	18
2	Quercetin	-6.1	1904	4	7
3	Rhoifolin	-10.2	3244	1	14
4	Adenosine A	-7.6	4410	45	10
5	Baicelein	-7.7	1904	4	5
6	Kaempferol	-7.9	4410	45	6
7	Pectolarin	-9.8	3244	1	15
8	Syringic acid	-6.0	1904	4	4
9	Epigallocatechin	-8.2	4410	5	7
10	Anthraquinone	-7.3	4410	5	2
11	Luteolin	-8.7	1904	4	6
12	Cynaroside	-9.4	3244	1	11
13	Caffeic acid	-6.0	3244	1	3
14	Gallic acid	-5.8	1904	4	4
15	Neochlorogenic acid	-8.2	3244	1	8
16	Isoquercetin	-9.4	3244	1	12
17	Benzoic acid	-5.7	1080	10	1
18	Tinnevellin glucoside	-8.4	3244	1	9
19	Rhein	-8.1	1174	1	5
20	Vanillic acid	-5.6	1080	4	3

TABLE 4.9: Ligands with Best Binding Score Values with 3CL Protease.

S.No	Ligands	HBD	LogP	M.W (g/mol)	Rotatable Bond
1	Senoside A	12	-1.0556	862.746	9
2	Quercetin	5	1.988	302.238	1
3	Rhoifolin	8	-1.0983	578.523	6
4	Adenosine A	5	-1.863	347.224	4
5	Baicelein	3	2.5768	270.24	1
6	Kaempferol	4	2.2824	286.239	1
7	Pectolinarin	7	-0.7867	622.576	8
8	Syringic acid	2	1.1076	198.174	3
9	Epigallocatechin	6	1.2517	306.27	1
10	Anthraquinone	0	2.462	208.216	0
11	Luteolin	4	2.2824	4	1
12	Cynaroside	7	-0.2445	448.38	4
13	Caffeic acid	3	1.1956	180.159	2
14	Gallic acid	4	0.501	170.12	1
15	Neochlorogenic acid	6	-0.6459	354.311	4
16	Isoquercetin	8	-0.5389	464.379	4
17	Benzoic acid	1	1.3848	122.123	1
18	Tinnevellin glucoside	5	0.2437	408.403	5
19	Rhein	3	1.5714	284.223	1
20	Vanillic acid	2	168.148	166.148	2

4.8 Interaction of Ligands and Targeted Protein

In Computational biology, LigPlot generates schematic 2D representation of protein-ligand complex, which facilitates the inspection of various enzyme complexes and demonstrates an informative and simple representation of the intermolecular interactions and their strength. These includes hydrogen bonds, hydrophobic interactions and atom accessibilities [62]. Analysis of docked complex (.pdb) was done by LigPlot, that generates automatically schematic diagrams of protein-ligand interactions for given PDB file [63]. 2D representations of 20 selected docked complexes were shown in Figure 4.4 to Figure 4.23. Hydrogen bonding and hydrophobic interactions among 3CL protease and selected twenty ligands were shown in Table 4.10.

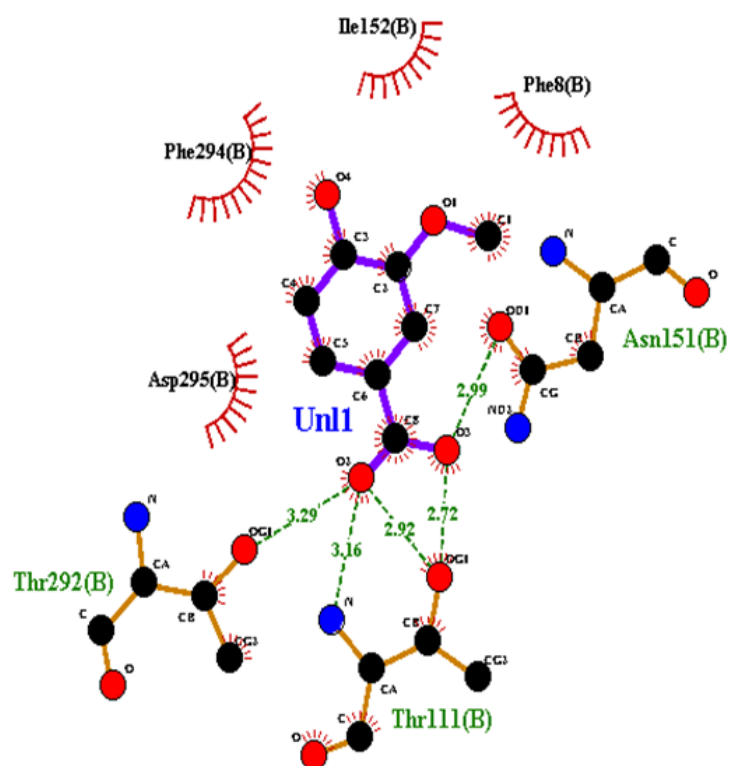


FIGURE 4.4: 2D Representation of Docked Complex Vanillic Acid-6M2N.

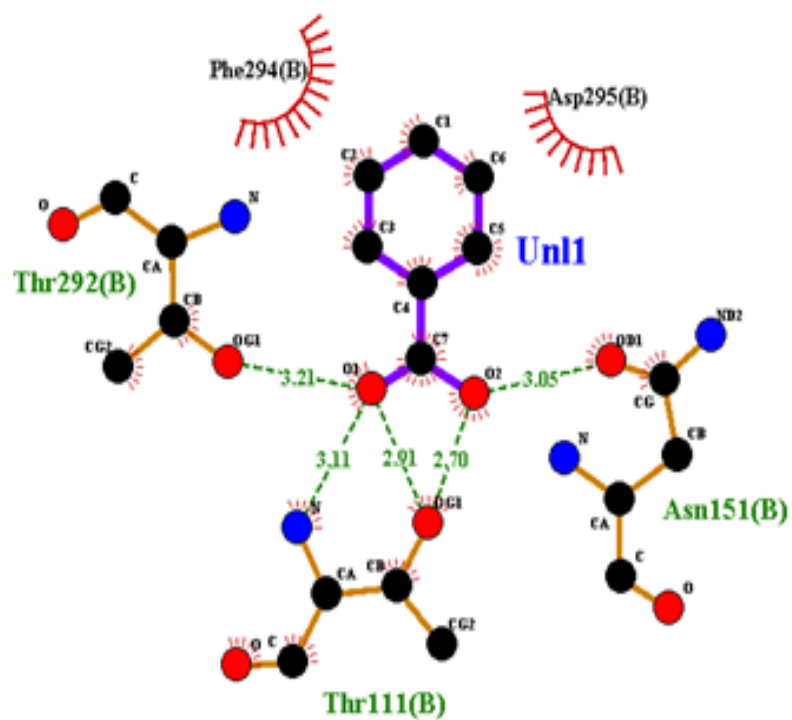


FIGURE 4.5: 2D Representation of Docked Complex of Benzoic Acid-6M2N

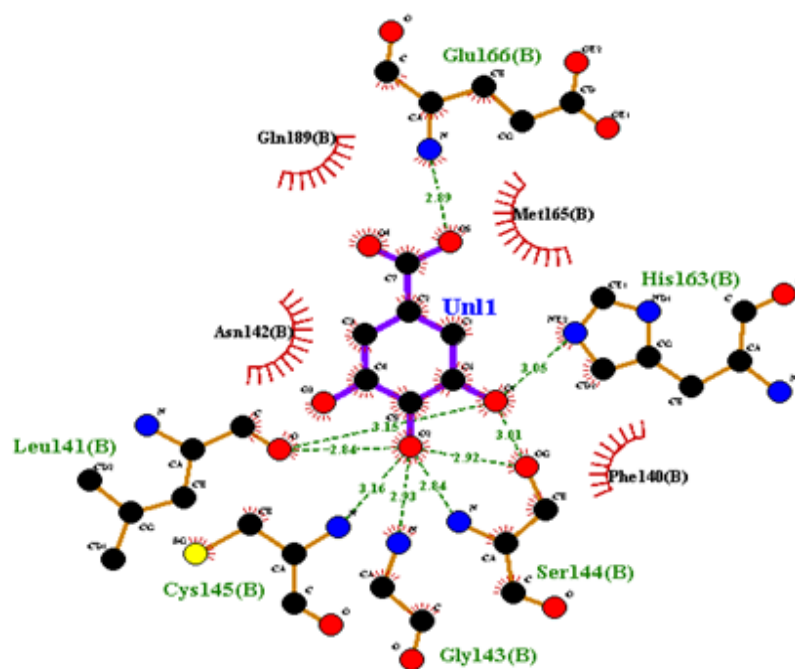


FIGURE 4.6: 2D Representation of Docked Complex of Gallic Acid-6M2N

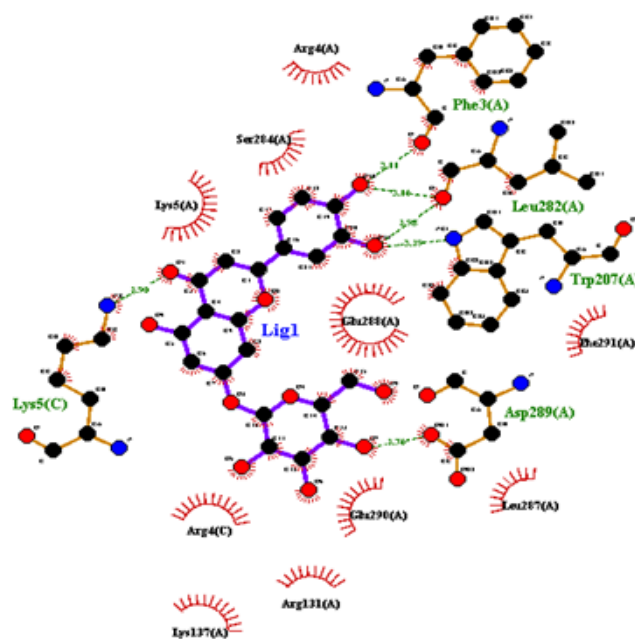


FIGURE 4.7: 2D Representation of Docked Complex Cynaroside-6M2N.

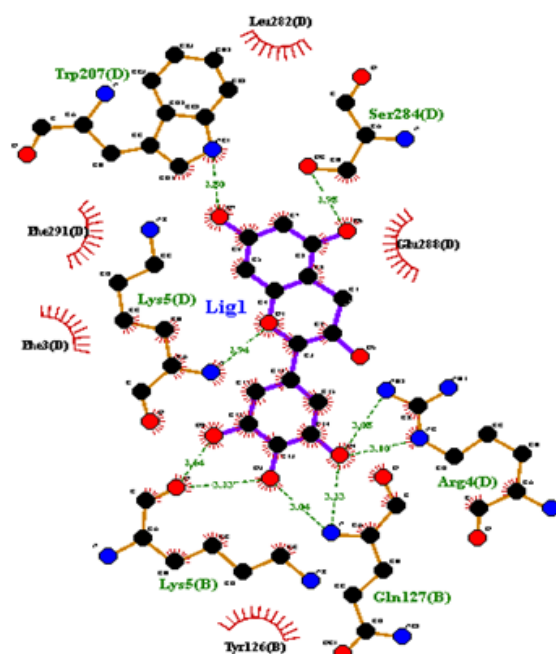


FIGURE 4.8: 2D Representation Docked Complex Epigallocatechin-6M2N.

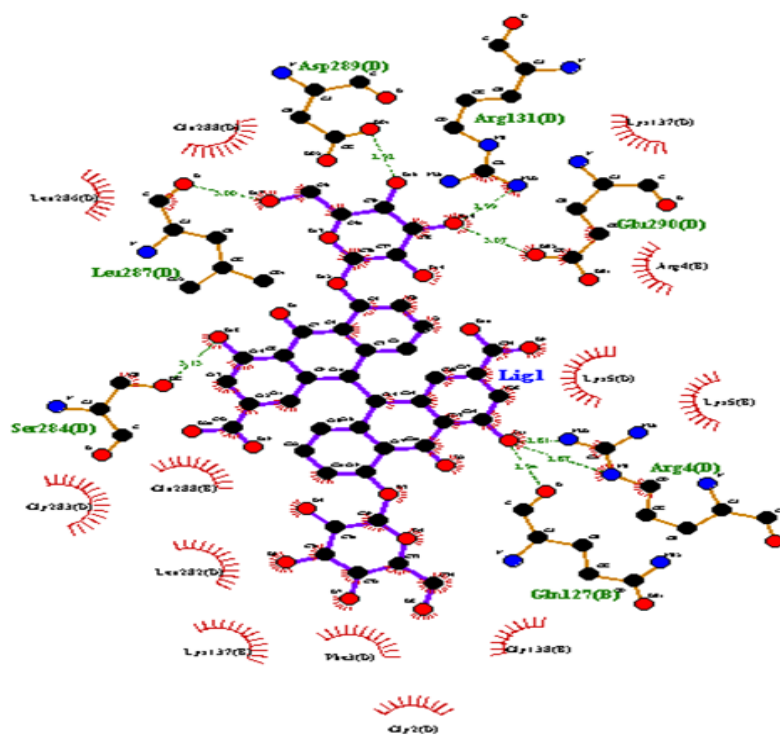


FIGURE 4.9: 2D Representation of Docked Complex Sennoside A-6M2N

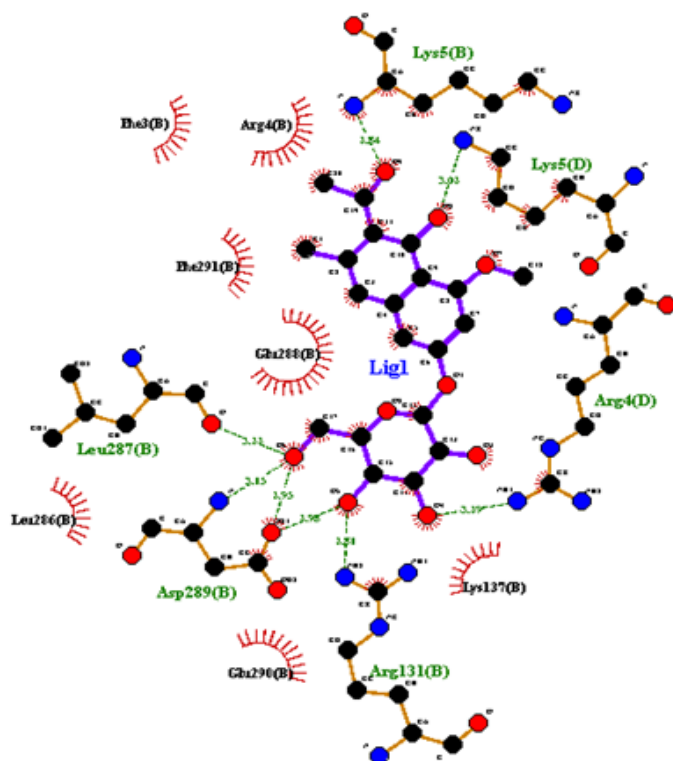


FIGURE 4.10: 2D Representation of Docked Complex Tinnevellingsucoside-6M2N.

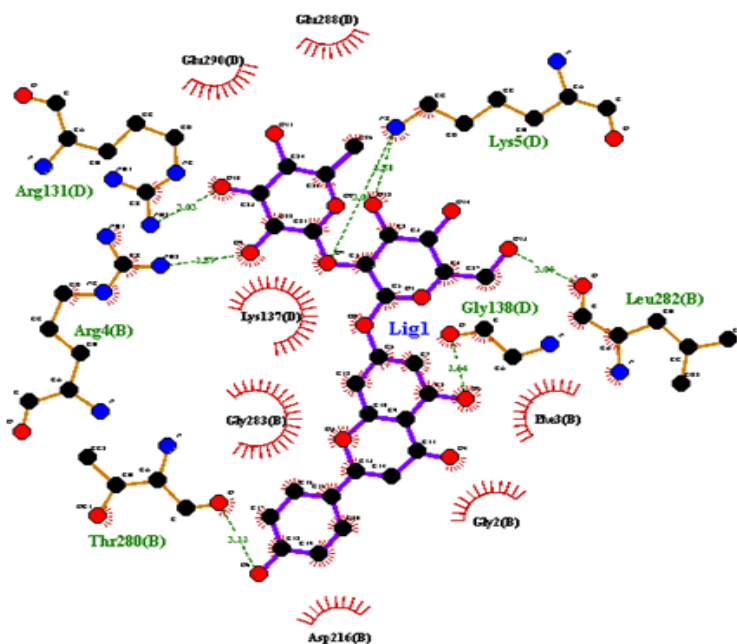


FIGURE 4.11: 2D Representation of Docked Complex Rhoifolin-6M2N.

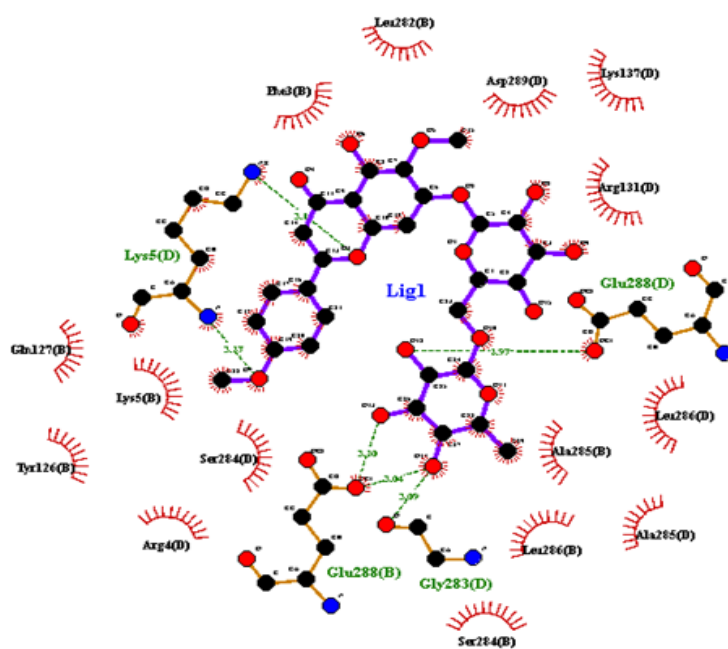


FIGURE 4.12: 2D Representation of Docked Complex Pectolinarin-6M2N.

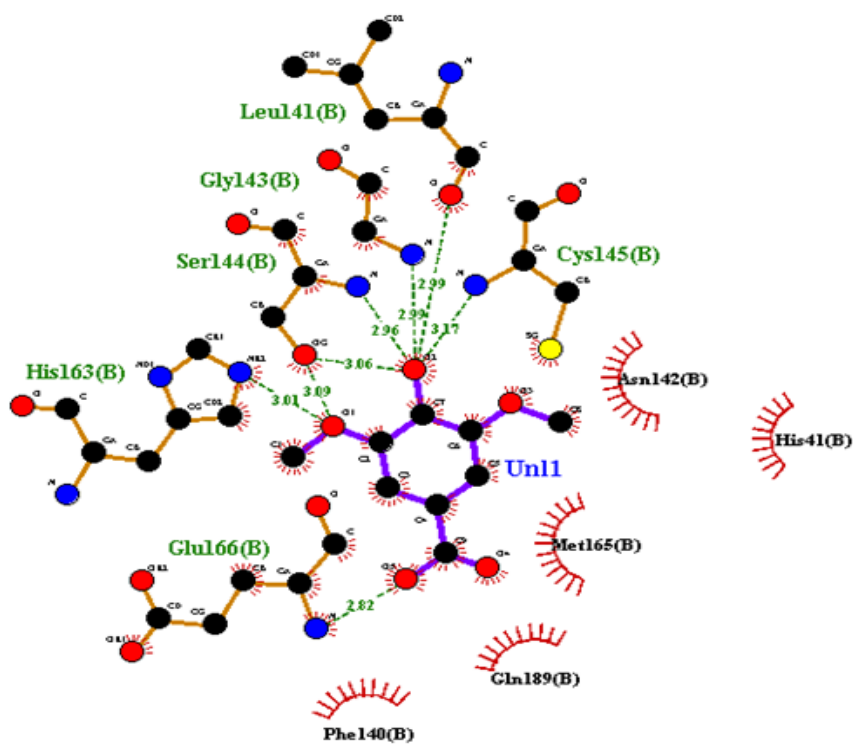


FIGURE 4.13: 2D Representation of Docked Complex Syringic Acid-6M2N.

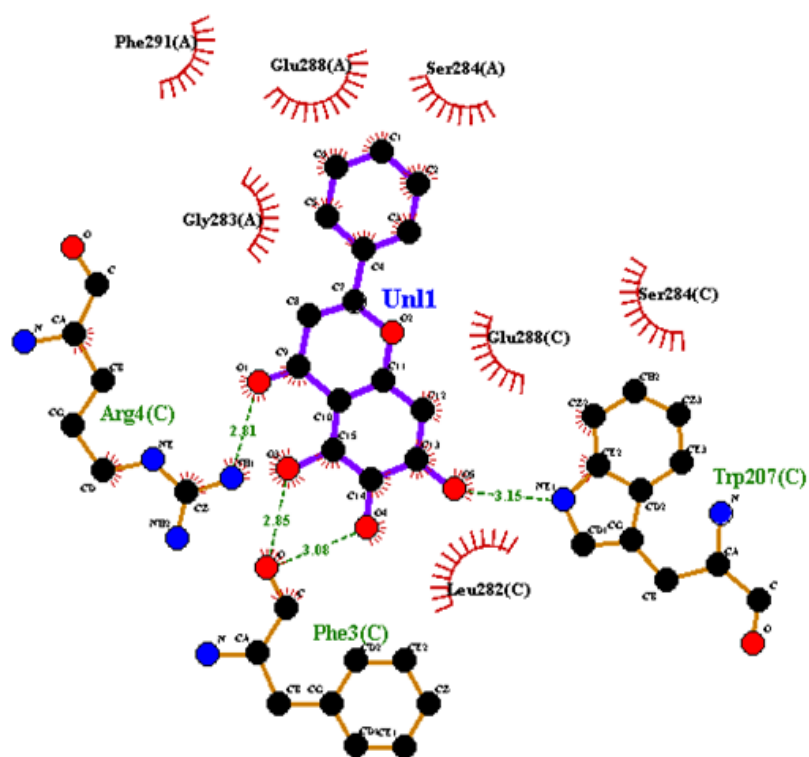


FIGURE 4.14: 2D Representation of Docked Complex Baicelein-6M2N.

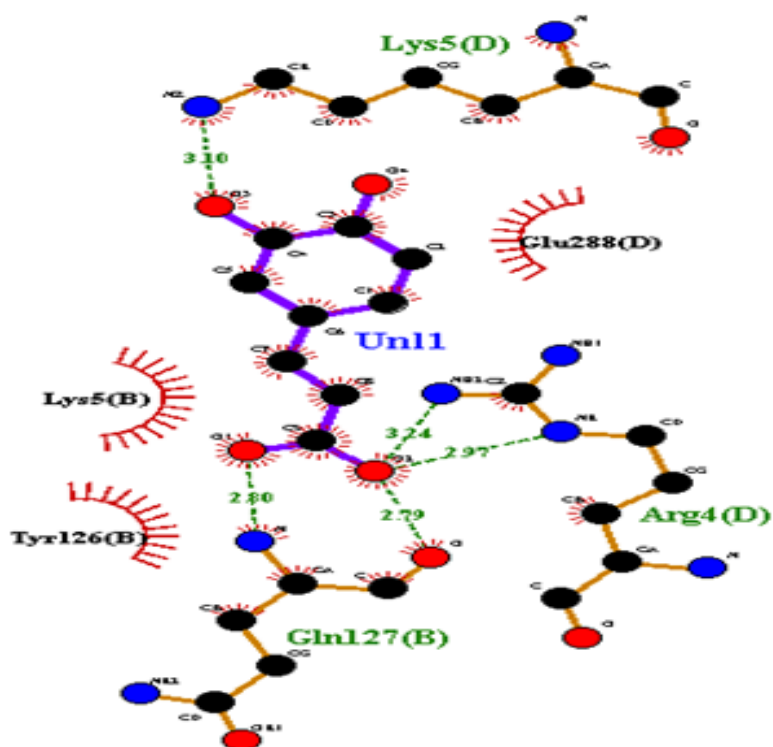


FIGURE 4.15: 2D Representation of Docked Complex Caffeic Acid-6M2N.

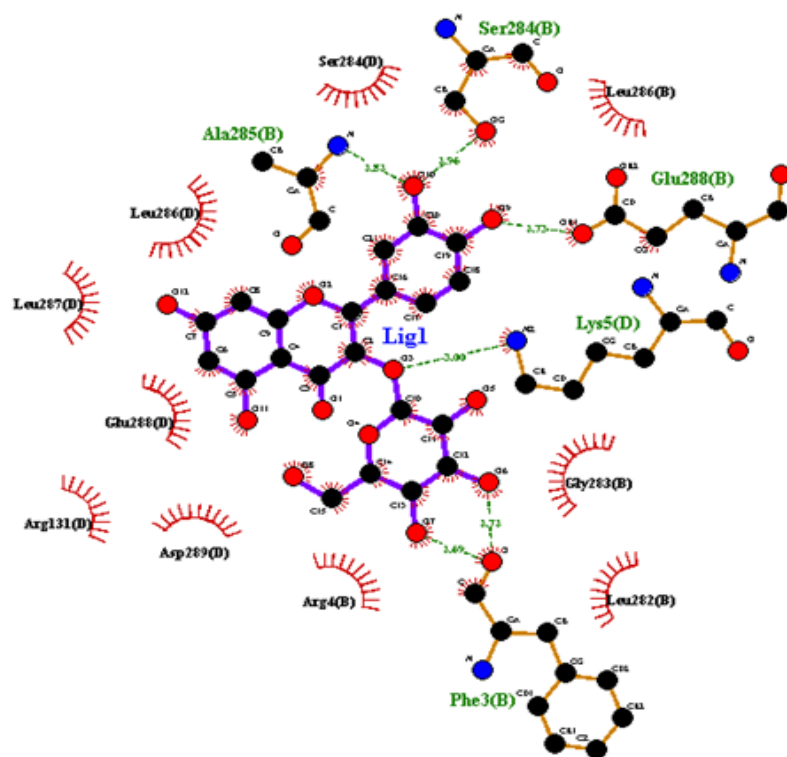


FIGURE 4.16: 2D Representation of Docked Complex Isoquercetin-6M2N.

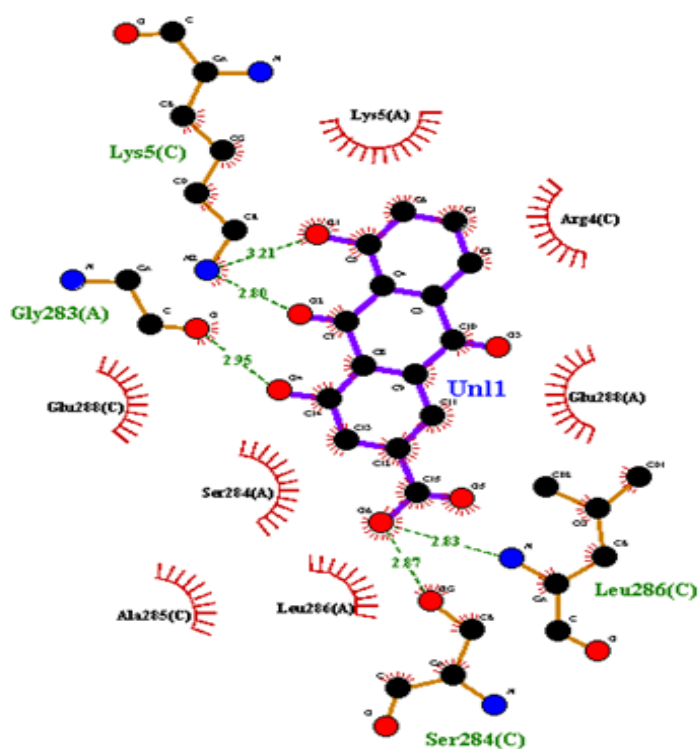


FIGURE 4.17: 2D Representation of Docked Complex Rhein-6M2N.

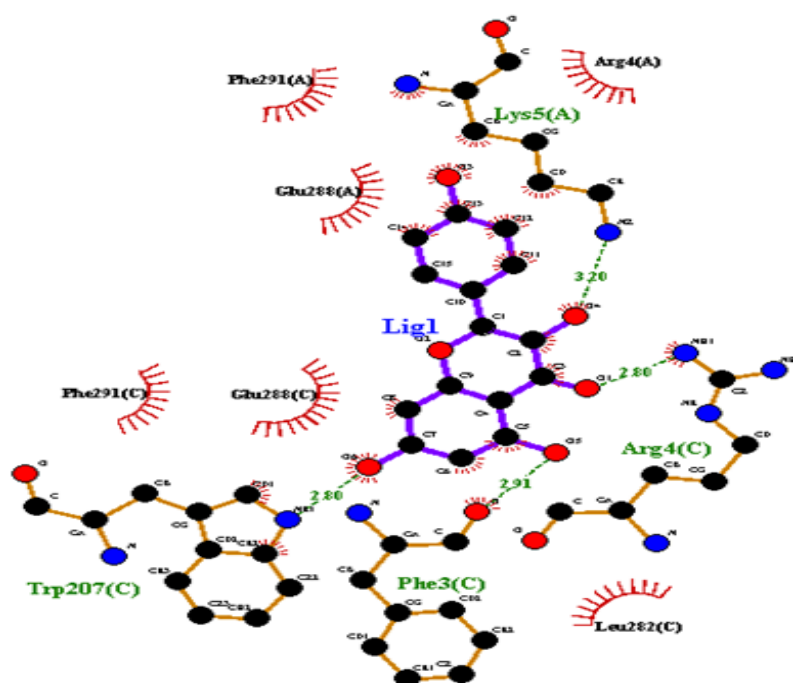


FIGURE 4.18: 2D Representation of Docked Complex Kaempferol-6M2N.

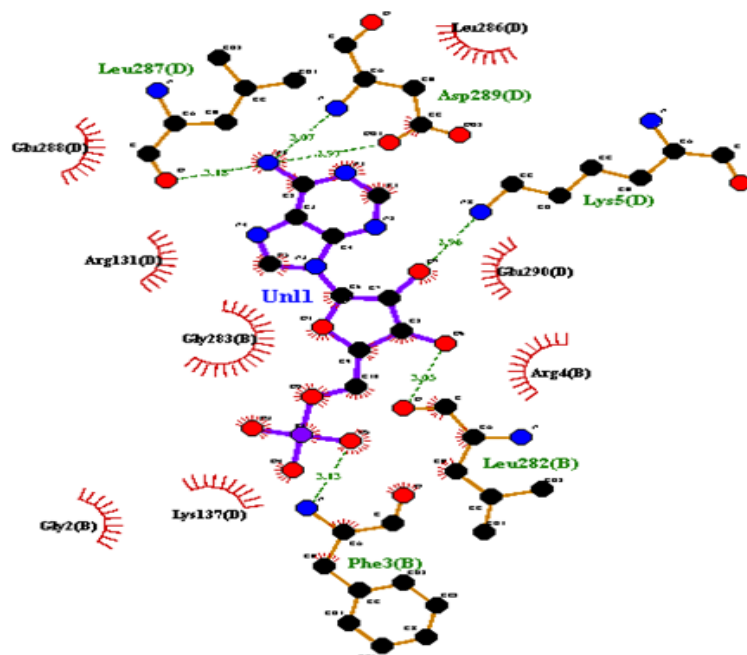


FIGURE 4.19: 2D Representation of Docked Complex Adenosine A-6M2N.

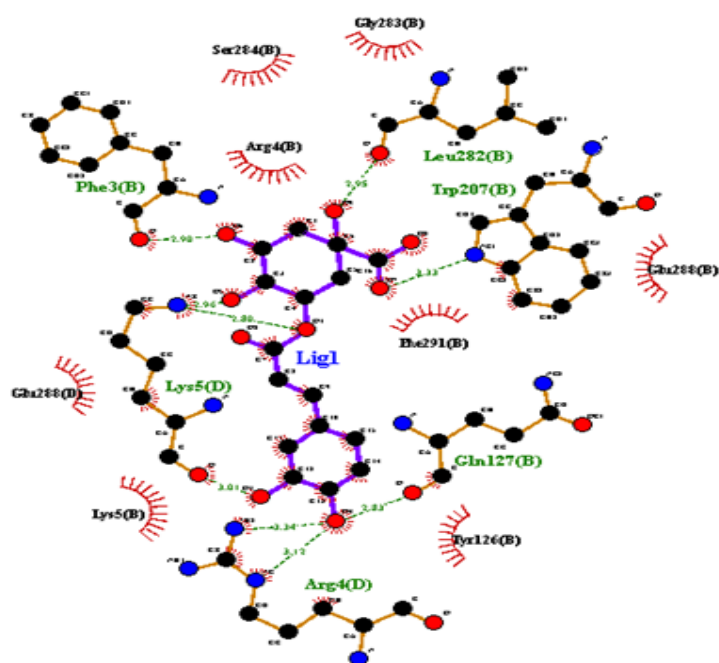


FIGURE 4.20: 2D Representation of Docked Complex Neochlorogenic Acid-6M2N.

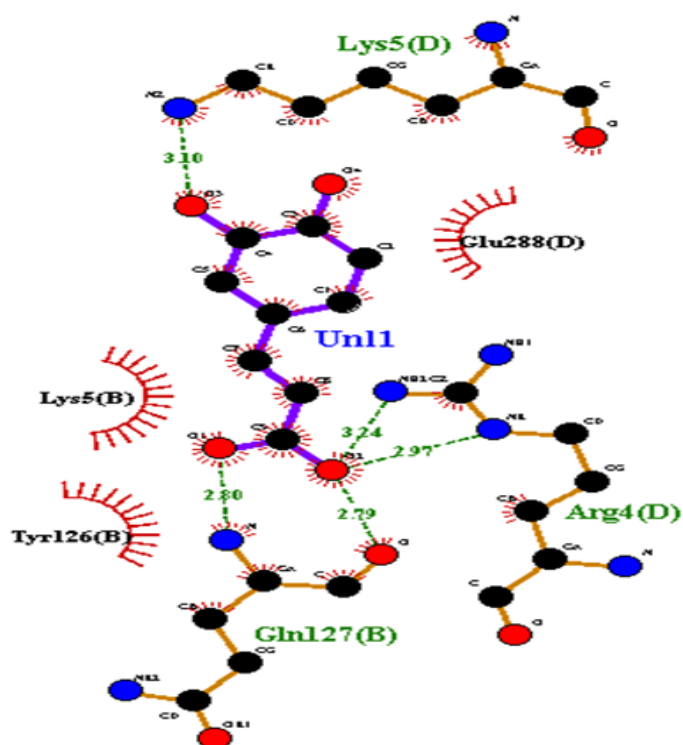


FIGURE 4.21: 2D Representation of Docked Complex Caffeic Acid-6M2N.

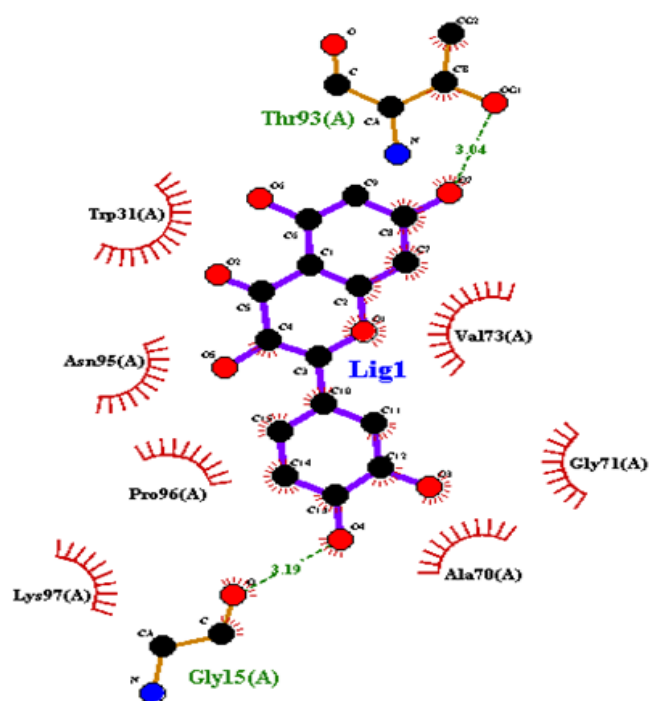


FIGURE 4.22: 2D Representation of Docked Complex Quercetin-6M2N.

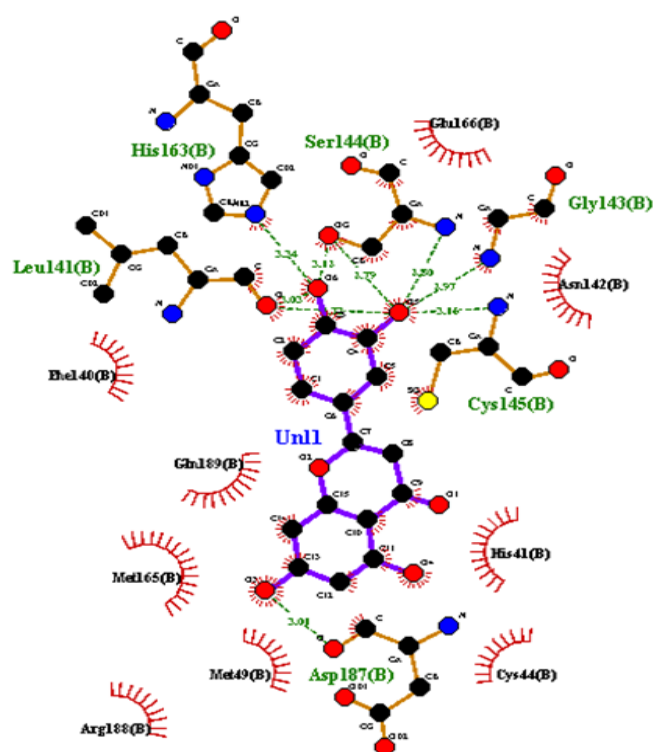


FIGURE 4.23: 2D Representation of Docked Complex Luteolin-6M2N.

TABLE 4.10: Active Ligand Showing Hydrogen and Hydrophobic Interactions

S.No	Ligands Name	Binding Energy	Hydrogen Bonding Amino Acids	Distance	Hydrophobic Bonding
1	Adenosine	-7.6	LUE287	3.18	LEU286
			ASP289	3.97	GLU288
			LYS5	2.96	ARG131
			LEU282	3.05	GLY283
			PHE3	3.13	GLU290
					ARG4
					GLY2
					LYS137
2	Sennoside A	-11.3	ASP289	1.91	GLU288
			ARG131	1.99	LEU286
			ARG131	1.99	LYS137
			LEU287	2.94	LEU137
			GLU290	2.99	GLY2
			SER284	3.13	LEU286
			ARG4	1.61	ARG4
			GLN127	1.9	LYS137
					LYS6

Continued Table 4.10: Active Ligand Showing Hydrogen and Hydrophobic Interactions

S.No	Ligands Name	Binding Energy	Hydrogen Bonding		Hydrophobic Bonding
			Amino Acids	Distance	
					PHE3
					GLY138
3	Rhoifolin	-10.2	ARG131	3.03	GLU290
			ARG4	2.59	GLU288
			THR280	3.22	LYS137
			LYS5	3.01	GLY283
			GLY138	2.64	PHE3
				3.06	GLY2
					ASP216
4	Quercetin	-6.1	THR93	3.04	TRP31
			GLY15	3.19	VAL73
				3.23	ASN95

Continued Table 4.10: Active Ligand Showing Hydrogen and Hydrophobic Interactions

S.No	Ligands Name	Binding Energy	Hydrogen Bonding		Hydrophobic Bonding
			Amino Acids	Distance	
					PRO96
					GLY138
					PRO96
					GLY71
					LYS97
					ALA70
5	Baicelein	-7.7	ARG4	2.81	PHE291
			PHE3	3.08	GLU288(A)
			TRP207	3.15	SER284
					GLY283
					GLU288(B)
					SER288
					LEU282

Continued Table 4.10: Active Ligand Showing Hydrogen and Hydrophobic Interactions

S.No	Ligands Name	Binding Energy	Hydrogen Bonding		Hydrophobic Bonding
			Amino Acids	Distance	
6	Kaempferol	-7.9	LYS5	3.20	PHE291
			ARG4	2.80	ARG4
			TRP204	2.80	GLU288(C)
			PHE3	2.91	PHE291
					GLU288(D)
7	Pectolinarin	-9.8	LYS5	3.27	LEU282
			GLU288(D)	3.20	PHE3
			GLY283	3.09	ASP289
			GLU288	2.97	LYS5
					ARG131
					LYS5
					GLN127

Continued Table 4.10: Active Ligand Showing Hydrogen and Hydrophobic Interactions

S.No	Ligands Name	Binding Energy	Hydrogen Bonding		Hydrophobic Bonding
			Amino Acids	Distance	
					SER284
					TYR126
					ARG4
					ALA285
					LEU286
					ARG131
					SER284(B)
8	Syringic acid	-6.0	LEU141	2.99	ASN142
			GLY143	2.96	HIS41
			SER144	3.09	MET165
			CYS145	3.17	GLN189
			HIS163	3.01	PHE140
			GLU166	2.82	

Continued Table 4.10: Active Ligand Showing Hydrogen and Hydrophobic Interactions

S.No	Ligands Name	Binding Energy	Hydrogen Bonding		Hydrophobic Bonding
			Amino Acids	Distance	
9	Epigallocatechin	-8.2	TRP207	2.50	LEU282
			SER284	2.98	GLU288
			LYS5	3.08	PHE3
			GLN127	3.23	TYR126
			ARG4	3.10	PHE291
10	Luteolin	-8.7	HIS163	3.34	GLU166
			SER144	3.13	PHE140
			LEU141	3.03	ASN142
			GLY143	2.97	GLN189
			CYS145	3.16	ARG168
			ASP187	3.01	MET49
					CYS44

Continued Table 4.10: Active Ligand Showing Hydrogen and Hydrophobic Interactions

S.No	Ligands Name	Binding Energy	Hydrogen Bonding		Hydrophobic Bonding
			Amino Acids	Distance	
11	Cynaroside	-9.4	PHE3	3.11	ARG4(A)
			LEU282	3.16	SER284
			TRP207	3.29	LYS5
			ASP289	2.76	GLY288
			LYS5	2.90	LEU287
					GLU290
					LYS137
					GLU288
12	Anthraquinone	-7.3	LYS5	3.07	GLU288(A)
			SER284	3.24	LYS5
					ARG4
					GLU288(C)
					TRP207

Continued Table 4.10: Active Ligand Showing Hydrogen and Hydrophobic Interactions

S.No	Ligands Name	Binding Energy	Hydrogen Bonding		Hydrophobic Bonding
			Amino Acids	Distance	
13	Gallic acid	-5.8	GLU166	2.89	GLN189
			HIS163	3.05	MET165
			LEU141	3.15	ASN142
			CYS145	3.16	PHE148
			SER144	3.01	
			GLY143	2.93	
14	Neochlorogenic acid	-8.2	LEU282	2.95	SER284
			PHE3	2.90	ARG4(B)
			TRP207	3.33	GLY283
			LYS5	2.80	GLU288(B)
			GLN127	2.83	TYR126
			ARG4	3.34	LYS5

Continued Table 4.10: Active Ligand Showing Hydrogen and Hydrophobic Interactions

S.No	Ligands Name	Binding Energy	Hydrogen Bonding		Hydrophobic Bonding
			Amino Acids	Distance	
15	Isoquercetin	-9.4	SER289	2.96	SER284
			ALA285	2.54	LEU286(B)
			GLU288	2.73	LEU286(D)
			LYS5	3.00	GLU288
			GLN127	2.72	LEU287
					GLU288
					GLY283
					ARG131
					ARG4
16	Benzoic acid	-5.7	THR292	2.81	PHE294
			THR111	3.08	ASP295
			ASN151	3.15	

Continued Table 4.10: Active Ligand Showing Hydrogen and Hydrophobic Interactions

S.No	Ligands Name	Binding Energy	Hydrogen Bonding		Hydrophobic Bonding
			Amino Acids	Distance	
17	Tinnevellin glucoside	-8.4	LYS5(B)	2.54	PHE3
			LYS5(D)	3.02	ARG4
			ARG(D)	3.29	PHE291
			LEU287	3.12	GLU288
			ASP289	2.95	LEU286
			ARG131	2.81	LYS137
18	Rhein	-8.1	LYS5	3.21	LYS5
			GLY283	2.95	ARG4
			LEU286	2.83	GLU288
			SER284	2.87	GLU288(C)
					GLU288(A)
					LEU286

Continued Table 4.10: Active Ligand Showing Hydrogen and Hydrophobic Interactions

S.No	Ligand Name	Binding Energy	Hydrogen Bonding		Hydrophobic Bonding
			Amino Acids	Distance	
19	Vanillic acid	-5.6	ASN151	2.99	ILE152
			THR292	3.29	PHE294
			THR111	3.16	PHE8 ASP295
20	Caffeic acid	-6.0	LYS5	3.10	GLU288
			ARG4	3.24	LYS5
			GLN127	2.80	TYR126

4.9 ADME Properties of Ligands

ADME properties of ligands were identified via pkCSM online tool by putting input (ligands) as SMILES. ADME properties describes the influence of drug level, kinetics and pharmacological activity of a compound that would be used as drug [64].

4.9.1 Absorption

In pharmacology, the transfer of a drug from administration site i.e. bloodstream to the action site or tissues is known as absorption [65]. Absorptive properties of selected compounds were given in Table 4.11 & 4.12.

TABLE 4.11: Absorptive Properties of Ligands.

S.No	Ligands	Water solubility	CaCO3 Permeability	Intestinal Absorption (human)	Skin Permeability
1	Sennoside A	-2.892	-1.874	0	-2.735
2	Quercetin	-2.925	-0.229	77.207	-2.735
3	Rhoifolin	-2.862	-0.942	24.308	-2.735
4	Adenosine A	-2.346	-0.596	61.243	-2.735
5	Baicelein	-3.302	1.117	94.268	-2.735
6	Kaempferol	-3.04	0.032	74.29	-2.735
7	Pectolinarin	-2.986	0.309	41.847	-2.735
8	Syringic acid	-2.223	0.495	73.076	-2.735
9	Epigallocatechin	-2.969	-0.375	54.128	-2.735
10	Anthraquinone	-3.435	1.31	99.057	-2.122
11	Luteolin	-3.094	0.096	81.13	-2.735
12	Cynaroside	-2.716	0.248	37.556	-2.735
13	Caffeic acid	-2.33	0.634	69.407	-2.722
14	Gallic acid	-2.56	-0.081	43.374	-2.735
15	Neochlorogenic acid	-2.449	-0.84	36.377	-2.735
16	Isoquercetin	-2.925	0.242	47.999	-2.735
17	Benzoic acid	-1.738	1707	100	-2.728
18	Tinnevellin glucoside	-2.494	-0.008	44.423	-2.739
19	Rhein	-2.843	-0.241	55	-2.735
20	Vanillic acid	-1.838	0.33	78.152	-2.726

TABLE 4.12: Absorptive Properties of Ligands.

S.No	Ligands	P-glyco Protein substrate	P-glyco protein-I inhibitor	P-glyco Protein II inhibitor
1	Sennoside A	Yes	No	No
2	Quercetin	Yes	No	No
3	Rhoifolin	Yes	No	No
4	Adenosine A	No	No	No
5	Baicelein	Yes	No	No
6	Kaempferol	Yes	No	No
7	Pectolinarin	Yes	No	No
8	Syringic acid	Yes	No	No
9	Epigallocatechin	Yes	No	No
10	Anthraquinone	No	No	No
11	Luteolin	Yes	No	No
12	Cynaroside	Yes	No	No
13	Caffeic acid	No	No	No
14	Gallic acid	No	No	No
15	Neochlorogenic acid	Yes	No	No
16	Isoquercetin	Yes	No	No
17	Benzoic acid	No	No	No
18	Tinnevellin glucoside	Yes	No	No
19	Rhein	Yes	No	No
20	Vanillic acid	No	No	No

4.9.2 Distribution

Pharmaceutical distribution refers to the transfer of a drug from one site to another in the body. After ingestion of the drug in systemic circulation through direct absorption or administration, it should be distributed into interstitial and intracellular fluid [66].

When a drug enters the systemic circulation by absorption or direct administration, it must be distributed into interstitial and intracellular fluids. The distribution properties of compounds was shown in Table 4.13.

TABLE 4.13: Distribution Properties of Ligands.

S.No	Ligands	VDss (human) (L/kg)	Fraction unbound (human)	BBB per- meability	CNS per- meability
1	Sennoside A	-0.369	0.312	-2.499	-5.848
2	Quercetin	1.559	0.206	-1.098	-3.065
3	Rhoifolin	1.14	0.152	-1.702	-4.798
4	Adenosine A	0.844	0.721	-1.23	-3.701
5	Baicelein	-0.004	0.156	-1.061	-2.21
6	Kaempferol	1.274	0.178	-0.939	-2.228
7	Pectolinarin	0.684	0.123	-1.863	-4.794
8	Syringic acid	-1.443	0.601	-0.191	-2.701
9	Epigallocatechin	1.301	0.274	-1.377	-3.507
10	Anthraquinone	0.232	0.136	0.372	-1.421
11	Luteolin	1.153	0.168	-0.907	-2.251
12	Cynaroside	0.884	0.224	-1.564	-3.93
13	Caffeic acid	-1.098	0.529	-0.647	-2.608
14	Gallic acid	-1.855	0.617	-1.102	-3.74
15	Neochlorogenic acid	-2.449	-0.84	36.377	-2.735
16	Isoquercetin	1.846	0.228	-1.688	-4.093
17	Benzoic acid	-1.64	0.523	-0.22	-2.002
18	Tinnevellin glucoside	-0.171	0.32	-1.364	-3.749
19	Rhein	-1.217	0.25	-0.807	-3.127
20	Vanillic acid	-1.739	0.518	-0.38	-2.628

4.9.3 Metabolism

Metabolism describes the catabolic and anabolic reactions of compounds in the body that are carried out through enzymes. Generally, metabolism occurs in the plasma of blood, liver, intestine and lungs [67]. Metabolism is the process of converting one compound into another with the help of enzymes.

Mostly metabolism occurs in the plasma of blood, liver, intestine and lungs. Generally, the metabolic process will convert the drug into a more water-soluble compound by increasing its polarity. The metabolic properties of selected compounds were shown in Table 4.14 & 4.15 respectively.

TABLE 4.14: Metabolic Properties of Ligands.

S.No	Ligands	CYP2D6 substrate	CYP3A4 substrate	CYP1A2 Inhibitor	CYP2C19 Inhibitor
1	Sennoside A	No	No	No	No
2	Quercetin	No	No	Yes	No
3	Rhoifolin	No	No	No	No
4	Adenosine A	No	No	No	No
5	Baicelein	No	No	Yes	No
6	Kaempferol	No	No	Yes	No
7	Pectolinarin	No	No	No	No
8	Syringic acid	No	No	No	No
9	Epigallocatechin	No	No	No	No
10	Anthraquinone	No	Yes	Yes	No
11	Luteolin	No	No	Yes	No
12	Cynaroside	No	No	No	No
13	Caffeic acid	No	No	No	No
14	Gallic acid	No	No	No	No
15	Neochlorogenic acid	No	No	No	No
16	Isoquercetin	No	No	No	No
17	Benzoic acid	No	No	No	No
18	Tinnevellin glucoside	No	No	No	No
19	Rhein	No	No	No	No
20	Vanillic acid	No	No	No	No

TABLE 4.15: Metabolic Properties of Ligands.

S.No	Ligands	CYP2C9 Inhibitor	CYP2D6 Inhibitor	CYP3A4 Inhibitor
1	Sennoside A	No	No	No
2	Quercetin	No	No	No
3	Rhoifolin	No	No	No
4	Adenosine A	No	No	No
5	Baicelein	Yes	No	No
6	Kaempferol	No	No	No
7	Pectolinarin	No	No	No
8	Syringic acid	No	No	No
9	Epigallocatechin	No	No	No
10	Anthraquinone	No	No	No
11	Luteolin	Yes	No	No
12	Cynaroside	No	No	No
13	Caffeic acid	No	No	No
14	Gallic acid	No	No	No
15	Neochlorogenic acid	No	No	No
16	Isoquercetin	No	No	No
17	Benzoic acid	No	No	No
18	Tinnevellin glucoside	No	No	No
19	Rhein	No	No	No
20	Vanillic acid	No	No	No

4.9.4 Excretion

In pharmacology excretion is a term that is used to describe removal of compounds and their metabolites through kidneys or in the feces. Excretion of drug occurs through three main sites: renal excretion via kidneys, fecal excretion via liver and gaseous excretion via lungs [68].

The organs involved in drug excretion are the kidneys, which play important role in excretion (renal excretion) and the liver (biliary excretion). Other organs may also be involved in excretion, such as the lungs for volatile or gaseous agents. Drugs can also be excreted in sweat, saliva and tears. Excretory properties of compounds was shown in Table 4.16.

TABLE 4.16: Excretory Properties of Ligands.

S.No	Ligands	Total clearance	Renal OCT2 substrate
1	Sennoside A	-0.889	No
2	Quercetin	0.407	No
3	Rhoifolin	-0.005	No
4	Adenosine A	0.763	No
5	Baicelein	0.252	No
6	Kaempferol	0.477	No
7	Pectolinarin	0.027	No
8	Syringic acid	0.646	No
9	Epigallocatechin	0.328	No
10	Anthraquinone	0.181	No
11	Luteolin	0.495	No
12	Cynaroside	0.478	No
13	Caffeic acid	0.508	No
14	Gallic acid	0.518	No
15	Neochlorogenic acid	0.307	No
16	Isoquercetin	0.394	No
17	Benzoic acid	0.707	No
18	Tinnevellin glucoside	0.321	No
19	Rhein	0.348	No
20	Vanillic acid	0.628	No

4.10 Lead Compound Identification

After detailed analysis of protein ligand interaction, binding score and pharmacokinetic properties of selected ligands, Luteolin is identified as the lead compound because it shows best binding score, hydrogen bonding and pharmacokinetic properties.

4.11 Selection of Antiviral Drug

The selection of the most effective antiviral drug depends on the physiochemical, ADMET properties and the mechanism of action with side effects. PubChem online database was used for physiochemical properties and pkCSM online tool was used for ADMET properties of drugs. Remdesivir is precursor of an adenosine triphosphate (ATP) analog, which has potential antiviral activity against COVID-19 that is caused by SARS-CoV-2. Remdesivir has FDA Emergency Authorization for use in adults and children with confirmed or suspected COVID-19 in hospitals with an $\text{SpO}_2 \leq 94\%$ [69]. Mechanism of action was identified by KEGG. Properties of antiviral drug Remdesivir was shown in Tables 4.17.

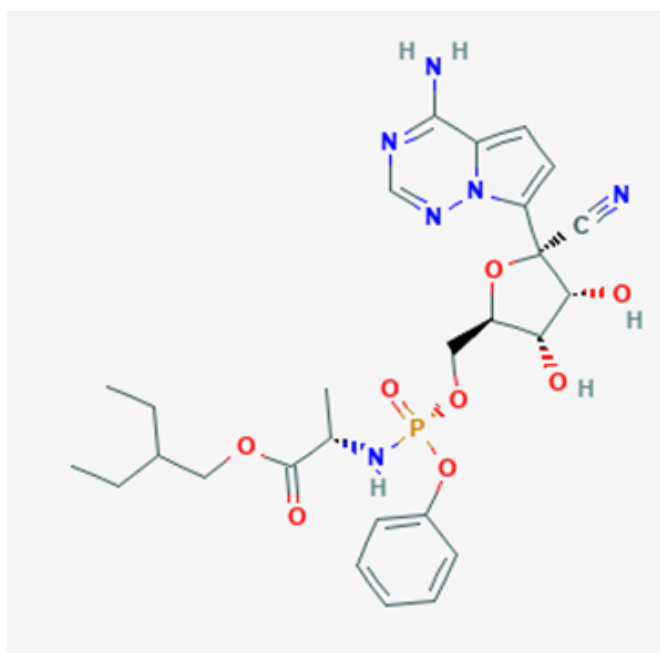


FIGURE 4.24: 2D Structure of Remdesivir Drug from Pubchem Database.

TABLE 4.17: This Table Shows Properties of Remdesivir.

S.No	Properties	Remdesivir
1	Chemical Formula	C ₂₇ H ₃₅ N ₆ O ₈ P
2	Molecular Weight	602.6 g/mol
3	Absorption	Approximately take 0.67-0.68 hours.
4	Water solubility	-
5	logP	2.312
6	H-bond donor	4
7	H-bond acceptor	13
8	Rotatable bond	13
9	Bioavailability	0
10	Polarizability	59.88A3
11	ADMET Probabil- ity	Not available
12	Side Effects	Low Blood Pressure, Nausea and Vomiting

4.12 ADMET Properties of Selected Drug

The ADMET properties of selected drug Remdesivir were identified by using online tool pkCSM. ADMET properties of Remdesivir were shown in Table 4.18 to 4.22 respectively.

TABLE 4.18: Toxicity prediction of Remdesivir

S.No	Model Name	Predicted values
1	Max.tolerated dose(human)	0.15
2	hERG I inhibitor	No
3	hERG II inhibitor	Yes
4	Oral rat acute toxicity	2.043
5	Oral rat chronic toxicity	1.639
6	Hepatotoxicity	Yes
7	Skin sensitization	No
8	t.pyriformis toxicity	0.285
9	Minnow toxicity	0.291

TABLE 4.19: Absorption values of Remdesivir.

S.No	Model Name	Value
1	Water solubility	-3.07
2	Caco2 permeability	0.635
3	Intestinal absorption (human)	71.109
4	Skin Permeability	-2.692
5	P-glycoprotein substrate	Yes
6	P-glycoprotein I inhibitor	Yes
7	P-glycoprotein II inhibitor	No

TABLE 4.20: Distribution Properties of Selected Drug Remdesivir

S.No	Model Name	Value
1	VDss (human)	0.307
2	Fraction unbound (human)	0.005
3	BBB permeability	-2.056
4	CNS permeability	-4.675

TABLE 4.21: Metabolic Properties of Remdesivir

S. No	Model Name	Predicted Value
1	CYP2D6 substrate	No
2	CYP3A4 substrate	Yes
3	CYP1A2 inhibitor	No
4	CYP2C19 inhibitor	No
5	CYP2C9 inhibitor	No
6	CYP2D6 inhibitor	No
7	CYP3A4 inhibitor	No

TABLE 4.22: Excretory Properties of Remdesivir

S.No	Model Name	Predicted Value
1	Total Clearance	0.198
2	Renal OCT2 substrate	No

4.13 Mechanism of Action of Remdesivir

KEGG database was used to identify mechanism of action of remdesivir. Through the action of carboxylesterase 1 or cathepsin A, remdesivir enters to cells before its monophosphate form is disrupted. It is then phosphorylated by unreported kinases to obtain its active triphosphate form remdesivir triphosphate (RDV-TP). The RDV-TP is effectively incorporated by the SARS-CoV-2 RdRp complex. Remdesivir provides a free 3-hydroxyl group that allows the chain length to be continuously increased.

Modelling and in vitro experiments show that at $i + 4$ (corresponding to the position of the fourth nucleotide incorporation after RDV-TP), the 1-cyano group involve in collision of remdesivir with Ser-861 of the RdRp, other enzyme prevent translocation and terminating replication at position $i + 3$ [70]. Remdesivir can target the RNA-dependent RNA polymerase (RdRp) and inhibit viral RNA synthesis. 3CLpro is an important CoV protease which is essential for cleavage of large replicase polyproteins during viral replication and can be targeted by many inhibitors.

4.14 Remdesivir Effects on Body

There is limited information regarding safety and effectiveness of using Remdesivir to treat patients of COVID-19. Remdesivir was firstly developed by manufacturers for hepatitis C, and later tried on the virus that causes Ebola. Some study results show that remdesivir may help some patients get better soon [71].

Beside these positive effects Remdesivir may cause some negative effects in body as nausea, vomiting, sweating and low blood pressure. In case of serious allergic reactions rash, itching, dizziness and difficulty in breathing may cause. During or after taking the dose of remdesivir, these side effects may occur such as serious headache, pounding in your neck or ears and facial swelling. The mention are the side effects of remdesivir drugs on the body.

4.15 Remdesivir Docking

CB Dock is online tool that was used for docking of Remdesivir (as ligand) and 3CLpro (as receptor). The result of docking was comprising of 5 best confirmational poses and finest is selected. Docking results of selected protein-ligand complex (6m2n-Remdesivir) were shown in Table 4.23. 2D representation of docked complex of 3CLpro and Remdesivir is shown in Figure 4.25.

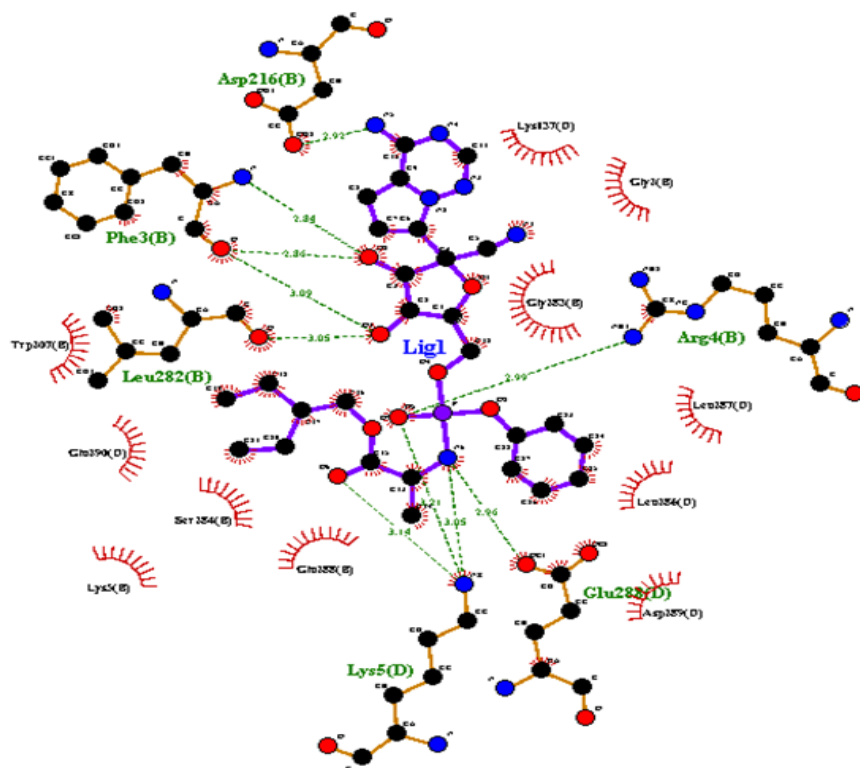


FIGURE 4.25: 2D Representation of Remdesivir and 3CLpro.

TABLE 4.23: Remdesivir Docking Scores Via Cb Dock

S.No	Properties	Values
1	Binding Score	-9.2
2	HBD	4
3	HBA	13
4	logP	2.312
5	Molecular Weight g/mol	602.6 g/mol
6	Rotatable Bonds	13
7	Grid Map	1
8	Cavity Size	3244

4.16 Comparison of Remdesivir and Luteolin

This comparison helps us to identify the better treatment for COVID-19. It is based on following parameters like; ADMET properties, binding affinity and physiochemical properties of Remdesivir and Luteolin. Lipinski rule of five of Remdesivir and Luteolin were shown in Table 4.24.

TABLE 4.24: Remdesivir and Luteolin Lipinski Rule of Fives

S.No	Drug	logP Value	Molecular Weight	H-Bond Acceptor	H-Bond Donor
1	Remdesivir	2.312	602.6 g/mol	13	4
2	Luteolin	2.2824	286.239 g/mol	6	4

So, it is determined that Luteolin compound shows better results than Remdesivir according to Lipinski rule of five's.

4.16.1 Comparison of ADMET Properties

ADMET properties comprises of values regarding to drug absorption, distribution, metabolism, excretion and toxicity. These values help us to determine the activity and efficiency of drugs. Comparison of ADMET properties were shown in Table 4.25 to 4.29.

TABLE 4.25: Comparison of Absorptive Properties of Remdesivir and Luteolin

S.No	Models	Remdesivir	Luteolin
1	Water solubility	-3.07	-3.094
2	Caco2 permeability	0.635	0.096
3	Intestinal absorption (human)	71.109	81.13
4	Skin Permeability	-2.735	-2.735
5	P-glycoprotein substrate	Yes	Yes
6	P-glycoprotein I inhibitor	Yes	No
7	P-glycoprotein II inhibitor	No	No

According to absorptive comparison, it is determined that intestinal absorption of Luteolin is more than Remdesivir and it is likely to P-glycoprotein inhibitor I. Water absorption and skin permeability is almost same in both compounds.

TABLE 4.26: Comparison of Distribution Properties of Remdesivir and Luteolin

S.No	Models	Remdesivir	Luteolin
1	VDss (human)	0.307	1.153
2	Fraction unbound (human)	0.005	0.168
3	BBB permeability	-2.056	-0.907
4	CNS permeability	-4.675	-2.251

VDss (Volume distribution in steady state) and fraction unbound in Luteolin is more than Remdesivir and BBB(Blood-brain barrier) permeability and CNS permeability values are greater in Remdesivir.

TABLE 4.27: Comparison of Metabolic Properties of Remdesivir and Luteolin

S.No	Models	Remdesivir	Luteolin
1	CYP2D6 substrate	No	No
2	CYP3A4 substrate	Yes	No
3	CYP1A2 inhibitor	No	Yes
4	CYP2C19 inhibitor	No	No
5	CYP2C9 inhibitor	No	Yes
6	CYP2D6 inhibitor	No	No
7	CYP3A4 inhibitor	No	No

Luteolin act likely CYP1A2 and CYP2C9 inhibitors and Remdesivir is metabolized like CYP3A4 substrate.

TABLE 4.28: Comparison of Excretory Properties of Remdesivir and Luteolin

S.No	Models	Remdesivir	Luteolin
1	Total Clearance	0.198	0.495
2	Renal OCT2 substrate	No	No

Total clearance value in Luteolin is more than Remdesivir.

TABLE 4.29: Comparison of Toxicity of Remdesivir and Luteolin

S.No	Model Name	Predict Values	
		Remdesivir	Luteolin
1	Max.tolerated dose(human)	0.15	0.499
2	hERG I inhibitor	No	No
3	hERG II inhibitor	Yes	No
4	Oral rat acute toxicity	2.043	2.455
5	Oral rat chronic toxicity	1.639	2.409
6	Hepatotoxicity	Yes	No
7	Skin sensitization	No	No
8	t.pyriformis toxicity	0.285	0.326
9	Minnow toxicity	0.291	3.169

The maximum tolerated dose (human), minnow toxicity and oral rate chronic toxicity in Luteolin is more than Remdesivir and Remdesivir is likely hERG II inhibitor.

4.16.2 Comparison of Docking Results and Physiochemical Properties

To find out activity manner and biochemical reactivity portion of drug we emphasized on comparison of physiochemical properties of Remdesivir and Luteolin. Comparison of docking values help to find best binding affinity of selected drugs. Comparison of Physiochemical Properties and Docking Scores of Remdesivir and Luteolin was shown in Table 4.30.

TABLE 4.30: Comparison of Physiochemical Properties and Docking Scores of Remdesivir and Luteolin.

S.No	Properties	Remdesivir	Luteolin
1	Binding Score	-9.2	-8.7
2	Cavity size	3244	1904
3	HBD	4	4
4	HBA	13	6
5	logP	2.312	2.282
6	Molecular Weight g/- mol	602.6 mol	286.239 g/mol
7	Molecular Formula	C ₂₇ H ₃₅ N ₆ O ₈ P	C ₁₅ H ₁₀ O ₆
8	Rotatable Bonds	13	1
9	Grid Map	1	4

According to Physiochemical properties it is determined that Luteolin is best compounds than Remdesivir as it is following Rule of five. Binding score and cavity size in Remdesivir is greater than Luteolin.

Chapter 5

Conclusions and Future Prospects

The aim of this study is to determine several bioactive compounds from *Senna alexandrina* those may be used to inhibit the activity of 3CLpro of SARS-CoV-2. Binding affinities of these compounds are as follows; Adenosine (-7.6), Sennoside A (-11.3), Rhoifolin (-10.2), Quercetin (-6.1), Baicelein (-7.7), Kaempferol (-7.9), Pectolinarin (-9.8), Syringic acid (-6.0), Epigallocatechin (-8.2), Luteolin (-8.7), Cynaroside (-9.4), Anthraquinone (-7.3), Gallic acid (-5.8), Neochlorogenic acid (-8.2), Isoquercetin (-9.4), Benzoic acid (-5.7), Tinnevellin glucoside (-8.4), Rhein(-8.1), Vanillic acid(-5.6) and Caffeic acid (-6.0).

Most of these compounds show effective binding scores, ADMET properties and low toxicity values. These compounds docked efficiently with 3CLpro and follow Lipinski rule of five. After detailed analysis of physiochemical properties, ADMET prediction, docking results and Lipinski rule of five, Luteolin is considered as lead compound. Comparison of Luteolin with the drug Remdesivir indicates that Luteolin is the most prescribed compound present in *Senna alexandrina* that can serve as a possible inhibitor of COVID-19 3CLpro. These findings suggest that Luteolin is considered as promising sign for development of antiviral medication for COVID-19. The information obtained from this present study may be used in future for the development of antiviral drug against COVID-19.

Bibliography

- [1]. Astuti, I. (2020). Severe Acute Respiratory Syndrome Coronavirus 2 (SARS-CoV-2): An overview of viral structure and host response. *Diabetes & Metabolic Syndrome: Clinical Research& Reviews*.
- [2]. Machhi, J., Herskovitz, J., Senan, A. M., Dutta, D., Nath, B., Oleynikov, M. D., & Kline, P. (2020). The natural history, pathobiology, and clinical manifestations of SARS-CoV-2 infections. *Journal of Neuroimmune Pharmacology*, 1-28.
- [3]. Huang, C., Wang, Y., Li, X., Ren, L., Zhao, J., Hu, Y., & Cheng, Z. (2020). Clinical features of patients infected with 2019 novel coronavirus in Wuhan, China. *The lancet*, 395(10223), 497-506.
- [4]. Shereen, M. A., Khan, S., Kazmi, A., Bashir, N.,& Siddique, R. (2020). COVID-19 infection: Origin, transmission, and characteristics of human coronaviruses. *Journal of Advanced Research*.
- [5]. Wang, H., Yang, P., Liu, K., Guo, F., Zhang, Y., Zhang, G., & Jiang, C. (2008). SARS coronavirus entry into host cells through a novel clathrin-and caveolae-independent endocytic pathway. *Cell research*, 18(2), 290-301.
- [6]. Qinfen, Z., Jinming, C., Xiaojun, H., Huanying, Z., Jicheng, H., Ling, F., & Jingqiang, Z. (2004). The life cycle of SARS coronavirus in Vero E6 cells. *Journal of medical virology*, 73(3), 332-337.
- [7]. Yang, Z. Y., Huang, Y., Ganesh, L., Leung, K., Kong, W. P., Schwartz, O., & Nabel, G. J. (2004). pH-dependent entry of severe acute respiratory syndrome

- coronavirus is mediated by the spike glycoprotein and enhanced by dendritic cell transfer through DC-SIGN. *Journal of virology*, 78(11), 5642-5650.
- [8]. Benarba, B., & Pandiella, A. (2020). Medicinal plants as sources of active molecules against COVID-19. *Frontiers in Pharmacology*.
- [9]. Boni, M. F., Lemey, P., Jiang, X., Lam, T. T. Y., Perry, B., Castoe, T., & Robertson, D. L. (2020). Evolutionary origins of the SARS-CoV-2 sarbecovirus lineage responsible for the COVID-19 pandemic. *bioRxiv*.
- [10]. Boni, M.F., Lemey, P., Jiang, X. et al. Evolutionary origins of the SARS-CoV-2 sarbecovirus lineage responsible for the COVID-19 pandemic. *Nat Microbiol* (2020).
- [11]. Riva, L., Yuan, S., Yin, X., Martin-Sancho, L., Matsunaga, N., Pache, L., & Chang, M. W. (2020). Discovery of SARS-CoV-2 antiviral drugs through large-scale compound repurposing. *Nature*, 1-11.
- [12]. Tiwari, V., Beer, J. C., Sankaranarayanan, N. V., Swanson-Mungerson, M., & Desai, U. R. (2020). Discovering small-molecule therapeutics against SARS-CoV-2. *Drug discovery today*.
- [13]. Zumla, A., Hui, D. S., Azhar, E. I., Memish, Z. A., & Maeurer, M. (2020). Reducing mortality from 2019-nCoV: host-directed therapies should be an option. *The Lancet*, 395(10224), e35-e36.
- [14]. Chaolin, H., Yeming, W., Xingwang, L., Lili, R., Jianping, Z., Yi, H., & Zhenshun, C. (2020). Clinical features of patients infected with 2019 novel coronavirus in Wuhan, China. *The Lancet*, 395(10223), 497-506.
- [15]. The, L. I. D. (2020). Challenges of coronavirus disease 2019. *The Lancet. Infectious Diseases*, 20(3), 261.
- [16]. Arabi, Y. M., Alothman, A., Balkhy, H. H., Al-Dawood, A., AlJohani, S., Al Harbi, S., & Al-Hameed, F. (2018). Treatment of Middle East respiratory

- syndrome with a combination of lopinavir-ritonavir and interferon- β 1b (Miracle trial): study protocol for a randomized controlled trial. *Trials*, 19(1), 1-13.
- [17]. Chen, Z. M., Fu, J. F., & Wang, Y. S. (2020). Diagnosis and treatment recommendations for pediatric respiratory infection caused by the 2019 novel coronavirus. *World journal of pediatrics*, 1-7.
- [18]. Namdeo, A. G. (2018). Cultivation of Medicinal and Aromatic Plants. In *Natural Products and Drug Discovery* (pp. 525-553). Elsevier.
- [19]. Benarba, B., & Pandiella, A. (2020). Medicinal plants as sources of active molecules against COVID-19. *Frontiers in Pharmacology*, 11.
- [20]. Hong-Zhi, D. U., Xiao-Ying, H. O. U., Yu-Huan, M. I. A. O., Huang, B. S., & Da-Hui, L. I. U. (2020). Traditional Chinese Medicine: an effective treatment for 2019 novel coronavirus pneumonia (NCP). *Chinese Journal of Natural Medicines*, 18(3), 206-210.
- [21]. Runfeng, L., Yunlong, H., Jicheng, H., Weiqi, P., Qin Hai, M., Yongxia, S., & Kui, Z. (2020). Lianhuaqingwen exerts anti-viral and anti-inflammatory activity against novel coronavirus (SARS-CoV-2). *Pharmacological research*, 104761.
- [22]. Yang, Y., Islam, M. S., Wang, J., Li, Y., & Chen, X. (2020). Traditional Chinese medicine in the treatment of patients infected with 2019-new coronavirus (SARS-CoV-2): a review and perspective. *International journal of biological sciences*, 16(10), 1708.
- [23]. Patten, G. S., Abeywardena, M. Y., & Bennett, L. E. (2016). Inhibition of angiotensin converting enzyme, angiotensin II receptor blocking, and blood pressure lowering bioactivity across plant families. *Critical Reviews in Food Science and Nutrition*, 56(2), 181-214.

- [24]. 24. Leelavathi, V., & Udayasri, P. Qualitative and Quantitative Analytical Studies for the Screening of Phytochemicals from the Leaf Extracts of *Senna alexandrina* Mill.
- [25]. Săvulescu, E., Georgescu, M. I., Popa, V., & Luchian, V. (2018, July). Morphological and Anatomical Properties of the *Senna Alexandrina* Mill. (*Cassia Angustifolia* Vahl.). In "Agriculture for Life, Life for Agriculture" Conference Proceedings (Vol. 1, No. 1, pp. 305-310). Sciendo.
- [26]. Roomi, M., Mahmood, M., & Khan, Y. (2020). Identifying Therapeutic Compounds Targeting RNA-Dependent-RNA-Polymerase of Sars-Cov-2.
- [27]. Morris, G. M., & Lim-Wilby, M. (2008). Molecular docking. In *Molecular modeling of proteins* (pp. 365-382). Humana Press.
- [28]. Dias, R., de Azevedo, J., & Walter, F. (2008). Molecular docking algorithms. *Current drug targets*, 9(12), 1040-1047.
- [29]. Li, J., Fu, A., & Zhang, L. (2019). An overview of scoring functions used for protein–ligand interactions in molecular docking. *Interdisciplinary Sciences: Computational Life Sciences*, 1-9.
- [30]. Fradera, X., & Mestres, J. (2004). Guided docking approaches to structure-based design and screening. *Current Topics in Medicinal Chemistry*, 4(7), 687-700.
- [31]. Dar, A. M., & Mir, S. (2017). Molecular docking: approaches, types, applications and basic challenges. *J Anal Bioanal Tech*, 8(2), 1-3.
- [32]. Muramatsu, T., Takemoto, C., Kim, Y. T., Wang, H., Nishii, W., Terada, T., & Yokoyama, S. (2016). SARS-CoV 3CL protease cleaves its C-terminal autoprocessing site by novel subsite cooperativity. *Proceedings of the National Academy of Sciences*, 113(46), 12997-13002.
- [33]. Yang, H., Yang, M., Ding, Y., Liu, Y., Lou, Z., Zhou, Z., & Gao, G. F. (2003). The crystal structures of severe acute respiratory syndrome virus

- main protease and its complex with an inhibitor. *Proceedings of the National Academy of Sciences*, 100(23), 13190-13195.
- [34]. He, J., Hu, L., Huang, X., Wang, C., Zhang, Z., Wang, Y., & Ye, W. (2020). Potential of coronavirus 3C-like protease inhibitors for the development of new anti-SARS-CoV-2 drugs: Insights from structures of protease and inhibitors. *International Journal of Antimicrobial Agents*, 106055.
- [35]. Konno, H., Wakabayashi, M., Takanuma, D., Saito, Y., & Akaji, K. (2016). Design and synthesis of a series of serine derivatives as small molecule inhibitors of the SARS coronavirus 3CL protease. *Bioorganic & medicinal chemistry*, 24(6), 1241-1254.
- [36]. Jo, S., Kim, S., Shin, D. H., & Kim, M. S. (2020). Inhibition of SARS-CoV 3CL protease by flavonoids. *Journal of enzyme inhibition and medicinal chemistry*, 35(1), 145-151.
- [37]. Park, J. Y., Ko, J. A., Kim, D. W., Kim, Y. M., Kwon, H. J., Jeong, H. J., & Ryu, Y. B. (2016). Chalcones isolated from *Angelica keiskei* inhibit cysteine proteases of SARS-CoV. *Journal of enzyme inhibition and medicinal chemistry*, 31(1), 23-30.
- [38]. Kumar, V., Tan, K. P., Wang, Y. M., Lin, S. W., & Liang, P. H. (2016). Identification, synthesis and evaluation of SARS-CoV and MERS-CoV 3C-like protease inhibitors. *Bioorganic & medicinal chemistry*, 24(13), 3035-3042.
- [39]. Wang, F., Chen, C., Tan, W., Yang, K., & Yang, H. (2016). Structure of main protease from human coronavirus NL63: insights for wide spectrum anti-coronavirus drug design. *Scientific reports*, 6, 22677.
- [40]. Qamar, M., Alqahtani, S., Alamri, M., & Chen, L. (2020). Structural basis of SARS-CoV-2 3CLpro and anti-COVID-19 drug discovery from medicinal Plants. Preprints, 2020030455.

- [41]. Ryu, Y. B., Jeong, H. J., Kim, J. H., Kim, Y. M., Park, J. Y., Kim, D., & Rho, M. C. (2010). Biflavonoids from *Torreya nucifera* displaying SARS-CoV 3CLpro inhibition. *Bioorganic & medicinal chemistry*, 18(22), 7940-7947.
- [42]. Gentile, D., Patamia, V., Scala, A., Sciortino, M. T., Piperno, A., & Rescifina, A. (2020). Putative inhibitors of SARS-CoV-2 main protease from a library of marine natural products: A virtual screening and molecular modeling study. *Marine drugs*, 18(4), 225.
- [43]. Das, S., Sarmah, S., Lyndem, S., & Singha Roy, A. (2020). An investigation into the identification of potential inhibitors of SARS-CoV-2 main protease using molecular docking study. *Journal of Biomolecular Structure and Dynamics*, (just accepted), 1-18.
- [44]. Viswanathan, S., & Nallamuthu, T. (2012). Phytochemical screening and antimicrobial activity of leaf extracts of *Senna alexandrina* Mill. against human pathogens. *International Journal of Current Science*, 2, 51-56.
- [45]. Roomi, M., Mahmood, M., & Khan, Y. (2020). Identifying Therapeutic Compounds Targeting RNA-Dependent-RNA-Polymerase of Sars-Cov-2.
- [46]. Tao, X. Q., Ke, Z. P., Zhang, X. Z., Deng, Y., Cao, Z. Y., Cao, L., & Xiao, W. (2020). Investigate mechanism of Jinzhen Oral Liquid for prevention COVID-19 based on network pharmacology and molecular docking technology. *Chin. Trad. Herbal Drugs*, 2326-2333.
- [47]. Heider, D., & Barnekow, A. (2008). DNA watermarks: A proof of concept. *BMC molecular biology*, 9(1), 40.
- [48]. Yuan, S., Chan, H. S., & Hu, Z. (2017). Using PyMOL as a platform for computational drug design. *Wiley Interdisciplinary Reviews: Computational Molecular Science*, 7(2), e1298.
- [49]. Wallace, A. C., Laskowski, R. A., & Thornton, J. M. (1995). LIGPLOT: a program to generate schematic diagrams of protein-ligand interactions. *Protein engineering, design and selection*, 8(2).

- [50]. Abid, K., Bari, Y. A., Younas, M., Tahir Javaid, S., & Imran, A. (2020). < covid19.> Progress of COVID-19 Epidemic in Pakistan. *Asia Pacific Journal of Public Health*, 1010539520927259.
- [51]. Gasteiger, E., Gattiker, A., Hoogland, C., Ivanyi, I., Appel, R. D., & Bairoch, A. (2003). ExPASy: the proteomics server for in-depth protein knowledge and analysis. *Nucleic acids research*, 31(13), 3784-3788.
- [52]. 52. Anand, K., Ziebuhr, J., Wadhwani, P., Mesters, J. R., & Hilgenfeld, R. (2003). Coronavirus main proteinase (3CLpro) structure: basis for design of anti-SARS drugs. *Science*, 300(5626), 1763-1767.
- [53]. Mostafa, S. I. (2007). Mixed ligand complexes with 2-piperidine-carboxylic acid as primary ligand and ethylene diamine, 2, 2'-bipyridyl, 1, 10-phenanthroline and 2 (2'-pyridyl) quinoxaline as secondary ligands: preparation, characterization and biological activity. *Transition Metal Chemistry*, 32(6), 769-775.
- [54]. Farabi, S., Ranjan Saha, N., Anika Khan, N., & Hasanuzzaman, M. (2020). Prediction of SARS-CoV-2 Main Protease Inhibitors from Several Medicinal Plant Compounds by Drug Repurposing and Molecular Docking Approach.
- [55]. Russell, B., Moss, C., George, G., Santaolalla, A., Cope, A., Papa, S., & Van Hemelrijck, M. (2020). Associations between immune-suppressive and stimulating drugs and novel COVID-19—a systematic review of current evidence. *ecancermedicalsecience*, 14.
- [56]. Garg, V. K., Avashthi, H., Tiwari, A., Jain, P. A., Ramkete, P. W., Kayastha, A. M., & Singh, V. K. (2016). MFPPi—multi FASTA ProtParam interface. *Bioinformatics*, 12(2), 74.
- [57]. Li, M., Ye, G., Si, Y., Shen, Z., Liu, Z., Shi, Y., & Peng, G. (2020). Structure of the Multiple Functional Domains from Coronavirus Nonstructural Protein 3. *Emerging Microbes & Infections*, 1-50.
- [58]. Hoffman, R. L., Kania, R. S., Brothers, M. A., Davies, J. F., Ferre, R. A., Gajiwala, K. S., & Lockner, J. W. (2020). Discovery of Ketone-Based

- Covalent Inhibitors of Coronavirus 3CL Proteases for the Potential Therapeutic Treatment of COVID-19. *Journal of medicinal chemistry*, 63(21), 12725-12747.
- [59]. Pires, D. E., Blundell, T. L., & Ascher, D. B. (2015). pkCSM: predicting small-molecule pharmacokinetic and toxicity properties using graph-based signatures. *Journal of medicinal chemistry*, 58(9), 4066-4072.
- [60]. Yeni, Y., Supandi Supandi, S., & Fajar, M. In silico toxicity prediction of 1-phenyl-1-(quinazolin-4-yl) ethanol compounds by using Toxtree, pkCSM and preADMET. In silico toxicity prediction of 1-phenyl-1-(quinazolin-4-yl) ethanol compounds by using Toxtree, pkCSM and preADMET, 8(2), 205-216.
- [61]. Liu, Y., Grimm, M., Dai, W. T., Hou, M. C., Xiao, Z. X., & Cao, Y. (2020). CB-Dock: a web server for cavity detection-guided protein–ligand blind docking. *Acta Pharmacologica Sinica*, 41(1), 138-144.
- [62]. Wallace, A. C., Laskowski, R. A., & Thornton, J. M. (1995). Ligplot: a program to generate schematic diagrams of protein-ligand interactions. *Protein engineering, design and selection*, 8(2), 127-134.
- [63]. Laskowski, R. A., & Swindells, M. B. (2011). LigPlot+: multiple ligand–protein interaction diagrams for drug discovery.
- [64]. Cheng, F., Li, W., Zhou, Y., Shen, J., Wu, Z., Liu, G., & Tang, Y. (2012). admetSAR: a comprehensive source and free tool for assessment of chemical ADMET properties.
- [65]. Kramer, C., Ting, A., Zheng, H., Hert, J., Schindler, T., Stahl, M., & Griffen, E. J. (2017). Learning medicinal chemistry absorption, distribution, metabolism, excretion, and toxicity (ADMET) rules from cross-company matched molecular pairs analysis (MMPA) miniperspective. *Journal of medicinal chemistry*, 61(8), 3277-3292.
- [66]. Norinder, U., & Bergström, C. A. (2006). Prediction of ADMET properties. *ChemMedChem: Chemistry Enabling Drug Discovery*, 1(9), 920-937.

-
- [67]. Alex, A. A., Beaumont, K., Kalgutkar, A., Walker, D., Dalvie, D., Prakash, C., & Miao, Z. (2010). Metabolism, pharmacokinetics and toxicity of functional groups: impact of chemical building blocks on ADMET. Royal Society of Chemistry.
- [68]. all, D. P., Stabenau, J. R., Zubrod, C. G., & Gaskins, J. (1959). Excretion of drugs between blood and cerebrospinal fluid: general methodology and effect of pH gradients. *Journal of Pharmacology and Experimental Therapeutics*, 125(3), 185-193.
- [69]. Beigel, J. H., Tomashek, K. M., Dodd, L. E., Mehta, A. K., Zingman, B. S., Kalil, A. C., & Lane, H. C. (2020). Remdesivir for the treatment of Covid-19—preliminary report. *The New England journal of medicine*.
- [70]. Tchesnokov, E. P., Feng, J. Y., Porter, D. P., & Götte, M. (2019). Mechanism of inhibition of Ebola virus RNA-dependent RNA polymerase by remdesivir. *Viruses*, 11(4), 326.
- [71]. Wang, Y., Zhang, D., Du, G., Du, R., Zhao, J., Jin, Y., & Wang, C. (2020). Remdesivir in adults with severe COVID-19: a randomised, double-blind, placebo-controlled, multicentre trial. *The Lancet*.